

# Significance tests of feature relevance for a blackbox learner

**Ben Dai**

BDAI@UMN.EDU

*School of Statistics  
University of Minnesota  
Minneapolis, MN 55455, USA*

**Xiaotong Shen**

XSHEN@UMN.EDU

*School of Statistics  
University of Minnesota  
Minneapolis, MN 55455, USA*

**Wei Pan**

PANXX014@UMN.EDU

*Division of Biostatistics  
University of Minnesota  
Minneapolis, MN 55455, USA*

## Abstract

An exciting recent development is the uptake of deep learning in many scientific fields, where the objective is seeking novel scientific insights and discoveries. To interpret a learning outcome, researchers perform hypothesis testing for explainable features to advance scientific domain knowledge. In such a situation, testing for a blackbox learner poses a severe challenge because of intractable models, unknown limiting distributions of parameter estimates, and high computational constraints. In this article, we derive two consistent tests for the feature relevance of a blackbox learner. The first one evaluates a loss difference with perturbation on an inference sample, which is independent of an estimation sample used for parameter estimation in model fitting. The second further splits the inference sample into two but does not require data perturbation. Also, we develop their combined versions by aggregating the order statistics of the  $p$ -values based on repeated sample splitting. To estimate the splitting ratio and the perturbation size, we develop adaptive splitting schemes for suitably controlling the Type I error subject to computational constraints. By deflating the *bias-sd-ratio*, we establish asymptotic null distributions of the test statistics and their consistency in terms of statistical power. Our theoretical power analysis and simulations indicate that the one-split test is more powerful than the two-split test, though the latter is easier to apply for large datasets. Moreover, the combined tests are more stable while compensating for a power loss by repeated sample splitting. Numerically, we demonstrate the utility of the proposed tests on two benchmark examples. Accompanying this paper is our Python library `dnn-inference` (<https://dnn-inference.readthedocs.io/en/latest/>) that implements the proposed tests.

**Keywords:** Adaptive splitting, combining, computational constraints, deep learning inference, feature relevance, power.

## 1. Introduction

Driven by recent advancements in deep learning (Schmidhuber, 2015), scientists demand accountability and interpretability beyond prediction accuracy. In particular, they seek answers to scientific questions, for example, if a specific brain region is functionally associated with Alzheimer’s disease. In this article, we develop tests for feature relevance of a blackbox

learner with an unknown feature distribution, subject to computational constraints when, for instance, only a limited number of repeated model fitting/training is permissible.

A deep learner (Schmidhuber, 2015) is often referred to as a blackbox, in which the learning process between input and output is mysterious due to the lack of knowledge about hidden patterns inside a neural net. A blackbox learner is trained to predict the outcome by minimizing a loss function. Yet, statistical inference for a blackbox learner remains understudied partly because of 1) the lack of understanding of a blackbox model, 2) the difficulty of deriving the limiting distribution of a test statistic, and 3) computational and statistical constraints for a blackbox model, that is, a large number of repeated training is prohibitive. For example, it is common to require excessive time for hundreds of machines to train a neural net (Goodfellow et al., 2016). Consequently, computationally intensive methods such as bootstrap (Efron, 1992), permutation (Ojala and Garriga, 2010), and conditional permutation (Berrett et al., 2019) become impractical, especially so for a complex neural net with massive data.

Given a random sample  $(\mathbf{X}_i, \mathbf{Y}_i)_{i=1}^N$  of sample size  $N$ , we test for a collection of hypothesized features  $\mathbf{X}_{\mathcal{S}} = \{X_j; j \in \mathcal{S}\}$ , subset of  $\mathbf{X} = (X_1, \dots, X_d)^\top$ , to be associated with the outcome  $\mathbf{Y} \in \mathbb{R}^K$  through an unspecified functional form, where  $\mathcal{S}$  is an index set for the hypothesized features and  $\mathbf{Y}$  is the outcome that could be a vector or scalar. A problem of this kind frequently occurs, for instance, in medical imaging such as a computerized tomography scan, where a region of interest is routinely examined and tested via a convolutional neural network (CNN) (Zhang et al., 1988) for abnormality. A similar situation occurs in automatic object recognition via a CNN, as discussed in Section 6.

### 1.1 Existing methods

In the existing literature, inference methods can be categorized into two groups: non-blackbox tests and blackbox tests. Non-blackbox tests, such as the Wald test (Fahrmeir et al., 2007) and likelihood-ratio test (King, 1989; Wasserman et al., 2020), perform hypothesis testing for discriminative features based on the asymptotic distribution of the corresponding parameters in a parametric model such as a linear model. While blackbox tests focus on model-free hypothesis testing, especially for deep neural networks, for example, Model-X knockoffs, conditional randomization tests (CRT; (Candès et al., 2018)) and holdout randomization test (HRT; (Tansey et al., 2018)). Specifically, Model-X knockoffs conduct variable selection with FDR control based on a specified variable importance measure on each of individual features. CRT and HRT examine the independence between the outcome and each individual feature conditional on the remaining features. The leave-one-covariate-out (LOCO; (Lei et al., 2018)) introduces the excess prediction error for each feature to measure its importance for a given dataset.

Despite the merits of the methods developed, they have their own limitations. First, for non-blackbox model, it is difficult to derive the asymptotic distribution of the parameter estimates from blackbox models, especially for over-parametrized neural networks. Moreover, the explicit feature-parameter correspondence may not be so straightforward for a blackbox model, such as a CNN using shared weights for spatial pixels, and a recurrent neural networks (RNN; (Rumelhart et al., 1986)) using shared weights for subsequent states. Second, most existing blackbox tests focus on variable importance or inference on a *single feature*,

yet a simultaneous test of a *collection* of features is more desirable in some applications. For example, in image analysis, it is more interesting to examine patterns captured by multiple pixels in a region, where the impact of every single pixel is negligible. Third, Model-X knockoffs, CRT and HRT generate samples from a known or estimated conditional feature distribution to construct a test statistic. However, the complete conditionals may not be easy to know or estimate in practice, especially for complex datasets such as image or text data. Finally, CRT requires massive computing to refit a model many times, which is infeasible for complex deep neural networks. More detailed discussion about the connections and differences between the existing tests and the proposed tests can be found in 2.5 and 6.1.

## 1.2 Our contributions

This article proposes a one-split and a two-split tests, addressing some gaps left by existing tests. Our main contributions are summarized as follows.

- A novel formulation of risk invariance as the null hypothesis based on a collection of hypothesized features is proposed in (1) for a general loss function, which measures the contribution of hypothesized features to prediction. Moreover, its relation to conditional independence tests is indicated in Lemma 1.
- We derive the one-split/two-split tests based on the differenced empirical loss with and without hypothesized features to assess their impacts on prediction and address the inflated *bias-sd-ratio* issue. Moreover, we further strengthen these tests by robust aggregation of the order statistics of their *p*-values based on repeated sample splitting. This aggregation not only stabilizes a test but also can compensate for a power loss due to sample splitting.
- Theoretically, we show that the one-split and two-split tests, as well as their combined tests, can control the Type I error while being consistent in terms of power; c.f. Theorems 2, 8, 4, and 10. Practically, we develop a “log-ratio” and “data-adaptive” sample splitting scheme to provide a reasonable splitting ratio and the perturbation size for suitably controlling the Type I error subject to computational constraints.
- Numerically, we demonstrate the differences between the proposed tests and other existing blackbox tests, and examine the utility of the proposed tests on various simulated examples and two real datasets in Section 6. In particular, we show that the standard one-split test without data perturbation leads to increasingly inflated Type I errors with larger datasets (c.f. Table 9).

This article is structured as follows. Section 2 introduces the one-split test as well as its combined test. Section 3 performs power analysis and establishes the consistency of these tests. Section 4 provides a theoretical example for illustration, followed by Section 5 that develops sample splitting schemes. Section 6 is devoted to simulation studies and an application to two benchmark examples, handwritten digit recognition with the well-known MNIST dataset and pneumonia diagnosis with a chest X-ray image dataset, to demonstrate the proposed tests’ performance and utility. The Appendix encompasses the two-split test’s results, additional numerical examples, and technical proofs.

## 2. Hypothesis testing for feature relevance

In machine learning, a statistical model predicts an outcome  $\mathbf{Y}$  based on some features  $\mathbf{X}$  of dimension  $d$ , where  $l(f(\mathbf{X}), \mathbf{Y})$  is a loss function measuring the discrepancy between the observed outcome  $\mathbf{Y}$  and its prediction  $f(\mathbf{X})$ , and  $f$  is a prediction function such as a deep neural network. Our objective is to test the relevance of a subset of features  $\mathbf{X}_{\mathcal{S}} = \{X_j : j \in \mathcal{S}\}$  to the prediction of  $\mathbf{Y}$  with an unknown form of the prediction function, where  $\mathcal{S}$  is an index set of hypothesized features and  $\mathbf{X}_{\mathcal{S}^c} = \{X_j : j \notin \mathcal{S}\}$  with  $\mathcal{S}^c$  indicating the complement set of  $\mathcal{S}$ . Note that  $\mathbf{X}_{\mathcal{S}}$  can be a collection of weak features in that none of these features is individually significant to prediction, but collectively they are. For example, in image analysis, the impact of each pixel is negligible but a pattern of a collection of pixels (e.g. in a region) may instead become salient.

To formulate the proposed hypothesis, we first define masked data  $(\mathbf{Z}, \mathbf{Y})$  by replacing  $\mathbf{X}_{\mathcal{S}}$  by some irrelevant values as  $\mathbf{Z}_{\mathcal{S}}$ , while  $\mathbf{Z}_{\mathcal{S}^c} = \mathbf{X}_{\mathcal{S}^c}$  remains intact. Ideally,  $\mathbf{Z}_{\mathcal{S}}$  can be any constant vector, for convenience,  $\mathbf{Z}_{\mathcal{S}} = \mathbf{0}$ . Then we use a differenced risk  $R(f^*) - R_{\mathcal{S}}(g^*)$  to measure the impact of  $\mathbf{X}_{\mathcal{S}}$  on the prediction of the outcome  $\mathbf{Y}$ , where  $f^* = \operatorname{argmin}_f R(f)$  and  $g^* = \operatorname{argmin}_g R_{\mathcal{S}}(g)$  are the optimal prediction functions in population,  $R(f) = \mathbb{E}(l(f(\mathbf{X}), \mathbf{Y}))$  and  $R_{\mathcal{S}}(g) = \mathbb{E}(l(g(\mathbf{Z}), \mathbf{Y}))$  are the corresponding risks, and  $\mathbb{E}$  is the expectation with respect to randomness.

To determine if  $\mathbf{X}_{\mathcal{S}}$  is functionally relevant to the prediction of  $\mathbf{Y}$ , consider null  $H_0$  and alternative  $H_a$  hypotheses:

$$H_0 : R(f^*) - R_{\mathcal{S}}(g^*) = 0, \quad \text{versus} \quad H_a : R(f^*) - R_{\mathcal{S}}(g^*) < 0. \quad (1)$$

Rejection of  $H_0$  suggests that the feature set  $\mathbf{X}_{\mathcal{S}}$  is relevant to the prediction of  $\mathbf{Y}$ . It is emphasized that in (1), the targets are the two true or population-level functions  $f^*$  and  $g^*$ , instead of their estimates (based on a given sample) as implemented in some existing tests.

In the next section, we demonstrate the relation between the proposed hypothesis and the independence hypothesis. More discussion about the differences from the hypotheses in HRT and LOCO can be found in Sections 2.5 and 6.1.

### 2.1 Connection to independence

This subsection illustrates the relationships among the risk invariance hypothesis in (1), marginal independence, and conditional independence; the latter two are defined as:

Marginal independence:  $\mathbf{Y} \perp \mathbf{X}_{\mathcal{S}}$ , conditional independence:  $\mathbf{Y} \perp \mathbf{X}_{\mathcal{S}} \mid \mathbf{X}_{\mathcal{S}^c}$ .

**Lemma 1** *For any loss function, conditional independent implies risk invariance, or*

$$\mathbf{Y} \perp \mathbf{X}_{\mathcal{S}} \mid \mathbf{X}_{\mathcal{S}^c} \implies R(f^*) - R_{\mathcal{S}}(g^*) = 0.$$

Moreover, if the cross-entropy loss  $l(f(\mathbf{X}), \mathbf{Y}) = -\mathbf{1}_{\mathbf{Y}}^{\top} \log(f(\mathbf{X}))$  is used in (1), then  $H_0$  is equivalent to conditional independence almost surely under the marginal distribution of  $\mathbf{X}$ , that is,

$$R(f^*) - R_{\mathcal{S}}(g^*) = 0 \iff \text{For any } y, \mathbb{P}\left(\mathbb{P}(\mathbf{Y} = y \mid \mathbf{X}_{\mathcal{S}}, \mathbf{X}_{\mathcal{S}^c}) = \mathbb{P}(\mathbf{Y} = y \mid \mathbf{X}_{\mathcal{S}^c})\right) = 1,$$

As suggested by Lemma 1, conditional independence always implies risk invariance, but they can be almost surely equivalent in some cases. Hence, at any significance level, a rejection of the null hypothesis of risk invariance implies a rejection of the null hypothesis of conditional independence. Yet, such a relationship does not exist for marginal independence. Next, we present three cases with disparate loss functions to illustrate their relationships.

*Case 1.* (Constant loss):  $l(f(\mathbf{X}), Y) = C$  for a real constant  $C$ .

*Case 2.* (The  $L_2$ -loss in regression):  $l(f(\mathbf{X}), Y) = \mathbb{E}(Y - f(\mathbf{X}))^2$  for  $Y \in \mathbb{R}$  and  $\mathbf{X} \in \mathbb{R}^d$ .

*Case 3.* (The cross-entropy loss in classification):  $l(f(\mathbf{X}), Y) = \mathbf{1}_Y^\top \log(f(\mathbf{X}))$  for  $Y \in \{1, \dots, K\}$  and  $\mathbf{X} \in \mathbb{R}^d$ .

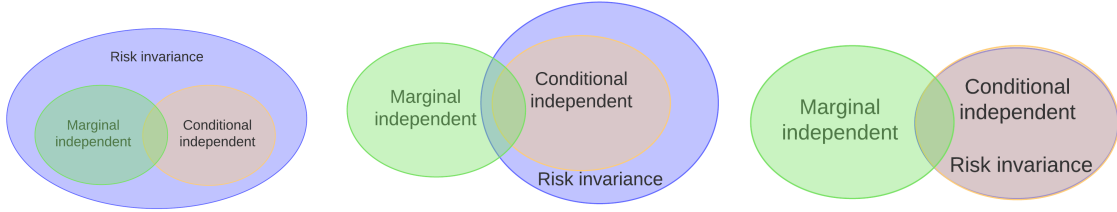


Figure 1: Three cases illustrate different relationships among marginal independence, conditional independence, and risk invariance.

As shown in Figure 1, conditional independence implies risk invariance in Cases 1 and 2 while they are equivalent in Case 3, as suggested by Lemma 1. On the other hand, marginal independence implies risk invariance in Case 1 instead of Cases 2 and 3. In general, conditional independence does not yield marginal independence and vice versa.

It is worthwhile mentioning that different loss functions can lead to different conclusions, as indicated by Lemma 1. In fact, we interpret a significance test according to the loss function being used. For example, consider the misclassification error (MCE) loss and the cross-entropy loss for testing the relevance of  $\mathbf{X}_S$  respectively. The  $H_0$  under the cross-entropy loss indicates that the hypothesized features are irrelevant to the conditional distribution of  $\mathbf{Y}$  given  $\mathbf{X}$ , yet the  $H_0$  under MCE suggests that the hypothesized features are irrelevant to classification accuracy.

## 2.2 One-split test

Given a dataset  $(\mathbf{X}_i, \mathbf{Y}_i)_{i=1}^N$ , we first split it into an estimation sample  $(\mathbf{X}_i, \mathbf{Y}_i)_{i=1}^n$  with  $n = \lfloor \zeta N \rfloor$  with  $\zeta$  indicating the splitting ratio and a non-overlapping inference sample  $(\mathbf{X}_j, \mathbf{Y}_j)_{j=n+1}^{n+m}$  with  $m = N - n$ ; that is, the two independent samples are respectively used for estimation and inference. The sample splitting intends to reduce the potential bias and to prevent overfitting, especially for an over-parametrized blackbox model, while simplifying the theory. The sample splitting strategy has been considered elsewhere for a different purpose in (Chernozhukov et al., 2018; Faraway, 1998; Wasserman and Roeder, 2009; Wasserman et al., 2020).

Given an estimation sample, we obtain an estimator  $(\hat{f}_n, \hat{g}_n)$  to approximate  $(f^*, g^*)$ , for example, by minimizing a regularized empirical loss of deep neural networks based on an estimation sample. Then, we examine the impact of hypothesized features on prediction

using the differenced empirical loss evaluated on an inference sample; that is,  $R(f^*) - R_S(g^*)$  is estimated by empirical evaluation of  $\hat{f}_n$  and  $\hat{g}_n$  on the inference sample  $(\mathbf{X}_j, \mathbf{Y}_j)_{j=n+1}^{n+m}$ .

One difficulty in inference is that under  $H_0$  the bias of  $R(\hat{f}_n) - R_S(\hat{g}_n)$  approximating  $R(f^*) - R_S(g^*)$  could dominate its standard error; that is, the ratio of the bias to the standard derivation, called the *bias-sd-ratio*, could be severely inflated, making the asymptotic distribution of  $R(\hat{f}_n) - R_S(\hat{g}_n)$  invalid for inference. This aspect is explained in detail in Section 2.4. To circumvent this difficulty, we present the one-split test with data perturbation to guard against the potentially inflated *bias-sd-ratio* by adding an independent noise:

$$\Lambda_n^{(1)} = \frac{\sum_{j=1}^m \Delta_{n,j}^{(1)}}{\sqrt{m\hat{\sigma}_n}}, \quad \Delta_{n,j}^{(1)} = l(\hat{f}_n(\mathbf{X}_{n+j}), \mathbf{Y}_{n+j}) - l(\hat{g}_n(\mathbf{Z}_{n+j}), \mathbf{Y}_{n+j}) + \rho_n \varepsilon_j, \quad (2)$$

where  $\hat{\sigma}_n^{(1)}$  is the sample standard deviation of  $\{\Delta_{n,j}^{(1)}\}_{j=1}^m$  given  $\hat{f}_n$  and  $\hat{g}_n$ ,  $\varepsilon_j \sim N(0, 1)$ ;  $j = 1, \dots, m$  are independent, and  $\rho_n > 0$  is the perturbation size. Note that our proposed test is in principle similar to classical hypothesis testing using a single test statistic. For example, if we use the negative log-likelihood as the loss function, it can be regarded as an extension of the likelihood ratio test (LRT; Buse (1982)) to a blackbox model.

According to the asymptotic null distribution of  $\Lambda_n^{(1)}$  in Theorem 2, we calculate the  $p$ -value  $P^{(1)} = \Phi(\Lambda_n^{(1)})$ , where  $\Phi(\cdot)$  is the cumulative distribution function of  $N(0, 1)$ .

Note that  $m$  is a subsequence of  $n$ , and  $m \rightarrow \infty$  as  $n \rightarrow \infty$ . To derive the asymptotic null distribution of  $\Lambda_n^{(1)}$ , we make the following assumptions.

**Assumption A** (Estimation consistency). For some constant  $\gamma > 0$ ,  $(\hat{f}_n, \hat{g}_n)$  satisfies

$$(R(\hat{f}_n) - R(f^*)) - (R_S(\hat{g}_n) - R_S(g^*)) = O_p(n^{-\gamma}), \quad (3)$$

where  $O_p(\cdot)$  denotes stochastic boundedness (Dodge and Commenges, 2006).

Assumption A concerns the rate of convergence in terms of the differenced regret, where  $R(\hat{f}_n) - R(f^*) \geq 0$ , known as the prediction regret with respect to a loss function  $l(\cdot, \cdot)$  of  $\hat{f}_n$ . Note that

$$R(\hat{f}_n) - R(f^*) - (R_S(\hat{g}_n) - R_S(g^*)) \leq \max(R(\hat{f}_n) - R(f^*), R_S(\hat{g}_n) - R_S(g^*)), \quad (4)$$

which says that the rate  $n^{-\gamma}$  is no worse than the least favorable one between the regrets of  $\hat{f}_n$  and  $\hat{g}_n$ . In the literature, the convergence rates for the right-hand of (4) has been extensively investigated. For example, the rate is  $n^{-\beta/(2\beta+d)}$  for nonparametric regression (Wasserman, 2006), and the rate is  $dn^{-2\beta/(2\beta+1)} \log^3 n$  for a regularized ReLU neural net (Schmidt-Hieber et al., 2020), where  $\beta$  is the degree of smoothness of a  $d$ -dimensional true regression function.

**Assumption B** (Lyapounov condition for  $\Lambda_n^{(1)}$ ). Assume that

$$m^{-\mu} \mathbb{E}(|\Delta_{n,1}^{(1)}|^{2(1+\mu)} | \mathcal{E}_n) \xrightarrow{p} 0, \quad \text{as } n \rightarrow \infty, \quad (5)$$

for some constant  $\mu > 0$ , where  $\Delta_{n,1}^{(1)}$  is defined in (2),  $\mathcal{E}_n = (\mathbf{X}_i, \mathbf{Y}_i)_{i=1}^n$  denotes an estimation sample, and  $\mathbb{E}(\cdot | \mathcal{E}_n)$  is the conditional expectation of the inference sample given  $\mathcal{E}_n$ .

**Assumption C** (Variance estimation) Assume that  $\text{Var}(\Delta_{n,1}^{(1)} | \mathcal{E}_n) \xrightarrow{p} (\sigma^{(1)})^2 > 0$  as  $n \rightarrow \infty$ , where  $\text{Var}(\cdot | \mathcal{E}_n)$  denotes the conditional variance of the inference sample given  $\mathcal{E}_n$ .

Assumptions B and C are used in applying the central limit theorem for triangle arrays (Cappé et al., 2006), where Assumption B is referred to as the Lyapounov condition (Cappé et al., 2006). Under some mild conditions,  $(\sigma^{(1)})^2 = \text{Var}(l(f^*(\mathbf{X}), \mathbf{Y}) - l(g^*(\mathbf{Z}(\mathbf{X})), \mathbf{Y})) + \rho_n^2 > 0$ , where  $\rho = \lim_{n \rightarrow \infty} \rho_n$ , c.f., Lemma 6.

The asymptotic null distribution for  $\Lambda_n^{(1)}$  is indicated in Theorem 2.

**Theorem 2 (Asymptotic null distribution of  $\Lambda_n^{(1)}$ )** *In addition to Assumptions A, B, and C, if  $m = o(n^{2\gamma})$ , then under  $H_0$ ,*

$$\Lambda_n^{(1)} \xrightarrow{d} N(0, 1), \quad \text{as } n \rightarrow \infty, \quad (6)$$

where  $\xrightarrow{d}$  denotes convergence in distribution.

Theorem 2 says that (6) is valid under an assumption of  $m = o(n^{2\gamma})$ , which restricts the sample splitting ratio. As a result, the estimation/inference sample ratio needs to be suitably controlled to ensure the validity of the proposed test. In Section 5, we propose a sample splitting scheme to estimate the splitting ratio to satisfy this assumption  $m = o(n^{2\gamma})$ , c.f., Lemma 7.

As an alternative, we present the two-split test in Appendix A to address the issue of *bias-sd-ratio*, where we divide an inference sample further into two equal subsamples for inference, in which no data perturbation is needed.

### 2.3 Combining p-values over repeated random splitting

Combining  $p$ -values of individual tests can strengthen the one-split test (2) via repeated random sample splitting. First, it stabilizes its result as in model averaging for prediction. Second, it can often compensate for the power loss by combining evidence across different split samples, as illustrated in our simulations in Section 6. As argued in Romano and DiCiccio (2019); Meinshausen et al. (2009), combining the results from multiple data splits is empirically more powerful than that from a single split. Subsequently, we use the order statistics of the  $p$ -values to combine the evidence from different splitting, though we could apply other types of combining such as the corrected arithmetic and geometric means (Vovk and Wang, 2018; Hardy et al., 1952).

Given a splitting ratio, we repeat the random splitting scheme  $U \geq 2$  times; that is, each time, we randomly split the original sample into an estimation sample of size  $n$  and an inference sample of size  $m$ . In practice,  $U$  cannot be large due to computational constraints and is usually 3-10 for large data applications. Then we compute the  $p$ -values  $P_u^{(1)}$  on the  $u$ -th split sample;  $u = 1, \dots, U$ , and combine them in two ways: the  $q$ -order and Hommel's weighted average of the order statistics (Hommel, 1983). Specifically,

$$\begin{aligned} (q\text{-order}) \quad \bar{P}^{(1)} &= \min\left(\frac{U}{q} P_{(q)}^{(1)}, 1\right), \\ (\text{Hommel}) \quad \bar{P}^{(1)} &= \min\left(C_U \min_{1 \leq q \leq U} \frac{U}{q} P_{(q)}^{(1)}, 1\right), \quad C_U = \sum_{q=1}^U \frac{1}{q}, \end{aligned} \quad (7)$$

where  $P_{(q)}^{(1)}$  is the  $q$ -th order statistic of  $P_1^{(1)}, \dots, P_U^{(1)}$ , with  $1 \leq q \leq U$  an integer.

The  $q$ -order combined test (7) is a generalized Bonferroni test with the Bonferroni correction factor  $\frac{U}{q}$ . The Hommel combined test renders robust aggregation and yields a better control of Type I error, where  $C_U$  is a normalizing constant.

In Theorem 3, we further generalize the result of Hommel (1983) to control the Type I error of the proposed tests asymptotically. In Theorem 5, we derive a power function bound for the combined test. A computational scheme for the combined tests is summarized in Algorithm 1.

**Theorem 3 (Type I error for the combined one-split test)** *Under Assumptions A-C, if  $m = o(n^{2\gamma})$ , then under  $H_0$ , for any  $0 < \alpha < 1$  and any  $U \geq 2$ , the combined one-split test for (2) achieves*

$$\lim_{n \rightarrow \infty} \mathbb{P}(\bar{P}^{(1)} \leq \alpha | H_0) \leq \alpha,$$

where  $\bar{P}^{(1)}$  is defined in (7).

## 2.4 Role of data perturbation

This subsection discusses the role of the data perturbation for the one-split test. Now consider the one-split test without perturbation, that is,  $\Lambda_n^{(1)}$  in (2) with  $\rho_n = 0$ . Then, we decompose  $\Lambda_n^{(1)}$  into three terms:

$$\begin{aligned} \Lambda_n^{(1)} &= \frac{\sqrt{m}}{\hat{\sigma}_n^{(1)}} \left( \frac{1}{m} \sum_{j=1}^m (\Delta_{n,j}^{(1)} - \mathbb{E}(\Delta_{n,j}^{(1)} | \mathcal{E}_n)) \right) + \frac{\sqrt{m}}{\hat{\sigma}_n^{(1)}} \left( R(\hat{f}_n) - R(f^*) - (R_S(\hat{g}_n) - R_S(g^*)) \right) \\ &\quad + \frac{\sqrt{m}}{\hat{\sigma}_n^{(1)}} (R(f^*) - R_S(g^*)) \equiv T_1 + T_2 + T_3. \end{aligned}$$

Under  $H_0$ ,  $T_3 = 0$ , and  $T_2$  is the *bias-sd-ratio* introduced in Section 2.2. Specifically, under  $H_0$ ,  $\hat{\sigma}_n^{(1)} \xrightarrow{p} 0$  as  $n \rightarrow \infty$  as opposed to  $\hat{\sigma}_n^{(1)} \xrightarrow{p} \sigma^{(1)} > 0$  in Assumption C when  $\rho_n = 0$ . As a result,  $T_1$  may not satisfy the assumption of the central limit theorem. Furthermore,  $T_2$  may not converge to zero. For example,  $T_2 = O_p(m^{1/2})$  when  $\hat{\sigma}_n^{(1)}$  and the differenced regret  $R(\hat{f}_n) - R(f^*) - (R_S(\hat{g}_n) - R_S(g^*))$  are vanishing in the same order. Thus, the asymptotic null distribution in (6) breaks down since  $\Lambda_n^{(1)}$  is dominated by  $T_2$ .

By comparison, when  $\rho_n \rightarrow \rho > 0$ ,  $(\sigma^{(1)})^2 = \text{Var}(l(f^*(\mathbf{X}), \mathbf{Y}) - l(g^*(\mathbf{Z}(\mathbf{X})), \mathbf{Y})) + \rho^2 > 0$ . By Assumption A,

$$|T_2| = \frac{\sqrt{m}}{\hat{\sigma}_n^{(1)}} \left| R(\hat{f}_n) - R_S(\hat{g}_n) - (R(f^*) - R_S(g^*)) \right| = O_p(m^{1/2} n^{-\gamma}),$$

which implies that  $T_2 \xrightarrow{p} 0$  under the assumption of  $m = o(n^{2\gamma})$ . Hence, the asymptotic null distribution of  $\Lambda_n^{(1)}$  in (6) is valid when  $\rho > 0$ . Moreover, a sample splitting method is proposed in (11), where the ratio condition  $m = o(n^{2\gamma})$  is automatically satisfied, as indicated in Lemma 7.

In later simulations (cf. Table 9), we will show numerically that, if no data perturbation is applied in the one-split test, it leads to increasingly inflated Type I errors with larger datasets in a neural network model.



## 2.5 Comparison with existing blackbox tests

The one-split test in (2) has some characteristics that distinguish it from other existing blackbox tests, including CRT (Candès et al., 2018), HRT Tansey et al. (2018), and LOCO tests (Lei et al., 2018).

CRT and HRT, can apply to test the conditional independence of a single feature individually to yield a  $p$ -value for every single feature. The LOCO test measures the increase in prediction error due to not using a specified feature in a given dataset. The differences between the proposed tests and other existing tests can be summarized in three folds. First, for CRT, HRT and LOCO tests, it is unclear how to test a set of multiple features  $\mathbf{X}_S$  simultaneously, which is the target of our tests. For instance, in image analysis, it is of more interest to examine patterns captured by multiple pixels in one or more regions, in which the impact of any single pixel is negligible. Second, the hypotheses for the tests are different. LOCO test conducts a significant test for the estimated model based on a given dataset with the mean absolute error, yet CRT, HRT and the proposed methods conduct testing at the population level; that is, the former two examines conditional independence, while the last one focuses on the risk invariance as specified in (1) based on a general loss function. Third, CRT and HRT require well-estimated conditional probabilities of every feature given the rest, which is often difficult in practice. Finally, the proposed tests are advantageous over CRT with reduced computational cost by avoiding a large number of model refitting.

## 3. Power analysis

This section performs power analysis of the one-split test (2) and its combined version (7).

Consider an alternative hypothesis  $H_a : R(f^*) - R_S(g^*) = -m^{-1/2}\delta < 0$  for  $\delta > 0$ . The power functions of the one-split test and its combined test can be written as

$$\pi_n(\delta) = \mathbb{P}(P^{(1)} \leq \alpha | H_a), \quad \bar{\pi}_n(\delta) = \mathbb{P}(\bar{P}^{(1)} \leq \alpha | H_a);$$

where  $\mathbb{P}(\cdot | H_a)$  denotes the probability under  $H_a$ , and  $\alpha > 0$  is the nominal level or level of significance.

Theorems 4 and 5 suggest that the one-split test and its combined test are consistent in that their asymptotic power tends to one as  $\delta \rightarrow \infty$ .

**Theorem 4 (Local limiting power of the one-split test)** *Suppose that the one-split test (2) satisfies Assumptions A-C and  $m = o(n^{2\gamma})$ , then*

$$\lim_{n \rightarrow \infty} \inf \pi_n(\delta) = \Phi\left(\frac{\delta}{\sigma(1)} - z_\alpha\right), \quad \text{and} \quad \lim_{\delta \rightarrow \infty} \liminf_{n \rightarrow \infty} \pi_n(\delta) = 1, \quad (8)$$

where  $z_\alpha = \Phi^{-1}(1 - \alpha)$  is the  $z$ -multiplier of the standard normal distribution.

Given the results of Theorem 10 in Appendix A, we note that the one-split test dominates the two-split test in terms of the asymptotic power.

**Theorem 5 (Local limiting power of the combined tests)** *Suppose that the one-split test (2) satisfies Assumptions A-C and  $m = o(n^{2\gamma})$ , then for  $\bar{P}^{(1)}$  defined as the  $q$ -order combined test in (7), we have*

$$\lim_{n \rightarrow \infty} \inf \bar{\pi}_n(\delta) \geq 1 - \min\left(\frac{U}{\alpha q} \Gamma, 1\right), \quad \lim_{\delta \rightarrow \infty} \lim_{n \rightarrow \infty} \inf \bar{\pi}_n(\delta) = 1,$$

and for  $\bar{P}^{(1)}$  defined as the Hommel combined test (7), we have

$$\lim_{n \rightarrow \infty} \inf \bar{\pi}_n(\delta) \geq 1 - \min\left\{\frac{C_U U}{\alpha q} \Gamma, 1; q = 1, \dots, U\right\}, \quad \lim_{\delta \rightarrow \infty} \lim_{n \rightarrow \infty} \inf \bar{\pi}_n(\delta) = 1,$$

where  $\Gamma = \Phi\left(\frac{-\delta}{\sqrt{2\sigma(1)}}\right) + \sqrt{\frac{q-1}{U-q+1}} \left(\Phi\left(\frac{\delta}{\sqrt{2\sigma(1)}}\right) - \Phi^2\left(\frac{\delta}{\sqrt{2\sigma(1)}}\right) - 2T\left(-\frac{\delta}{\sqrt{2\sigma(1)}}, \frac{\sqrt{3}}{3}\right)\right)^{1/2}$  and  $T(h, a) = \frac{1}{2\pi} \int_0^a \frac{\exp(-h^2(1+x^2)/2)}{x^2+1} dx$  is Owen's  $T$  function (Owen, 1956).

Note that the lower bounds in Theorem 5 can be further improved if the explicit dependency structures of the  $p$ -values from repeated sample splitting are known.

#### 4. Theoretical example

This section provides a specific theoretical example to illustrate the one-split test, and verify Assumptions A-C. Consider nonparametric regression,

$$Y = f^*(\mathbf{X}) + \epsilon, \quad \epsilon \sim N(0, \varsigma^2), \quad (9)$$

where  $f^*(\mathbf{x})$  is an unknown function on  $\mathbf{x} \in [-1, 1]^d$ . It is known that  $f^*(\mathbf{x}) = g^*(\mathbf{z})$  only depends on a subset of features of  $\mathbf{x}$ , in which  $\mathbf{z}_{\mathcal{S}_0} = \mathbf{0}$  and  $\mathbf{z}_{\mathcal{S}_0^c} = \mathbf{x}_{\mathcal{S}_0^c}$  with  $\mathcal{S}_0 = \{1, \dots, |\mathcal{S}_0|\}$ . Given a hypothesized index set  $\mathcal{S}$ , our goal is to test if  $\mathbf{X}_{\mathcal{S}}$  is relevant to predicting the outcome  $Y$ , as specified in (1).

For illustration, consider  $f^*(\mathbf{x}) = A((\mathbf{W}^L)^* A((\mathbf{W}^{L-1})^* \dots A((\mathbf{W}^1)^* \mathbf{x})))$ , where  $A(\cdot)$  is the ReLU activation function,  $(\mathbf{W}^l)^* = ((w_{ij}^l)^*) \in \mathbb{R}^{d_l \times d_{l-1}}$  is a weight matrix,  $\|(\mathbf{w}_j^l)^*\|_2 = \tau/d_{l-1}^{1/2}$ ,  $(\mathbf{w}_j^l)^*$  is the  $j$ -th column of the matrix  $(\mathbf{W}^l)^*$ ,  $\tau > 0$  is a constant,  $d_l$  is the width for the  $l$ -th layer, and  $d_0 = d$ ,  $d_L = 1$ ,  $d_1 = \dots = d_{L-1} = \varpi$  and  $L$  is the depth of the network. Clearly,  $f^* \in \mathcal{H}$ , where  $\mathcal{H}$  is defined as:

$$\mathcal{H} = \{f(\mathbf{x}) = A(\mathbf{W}^L A(\mathbf{W}^{L-1} \dots A(\mathbf{W}^1 \mathbf{x}))) : \|\mathbf{W}^l\|_2 \leq \tau, \|\mathbf{W}^l\|_{2,1} \leq \tau\}.$$

Given an estimation sample  $(\mathbf{X}_i, Y_i)_{i=1}^n$  and an inference sample  $(\mathbf{X}_j, Y_j)_{j=n+1}^{n+m}$ , consider a loss function  $l(\hat{y}, y) = (\hat{y} - y)^2$ , where  $\hat{y}$  is the predicted outcome of  $y$  and the prediction functions  $(\hat{f}_n, \hat{g}_n)$  are obtained:

$$\hat{f}_n = \operatorname{argmin}_{f \in \mathcal{H}} n^{-1} \sum_{i=1}^n l(f(\mathbf{X}_i), Y_i); \quad \hat{g}_n = \operatorname{argmin}_{g \in \mathcal{H}} n^{-1} \sum_{i=1}^n l(g(\mathbf{Z}_i), Y_i). \quad (10)$$

To solve (10), we apply a stochastic gradient descent (SGD) algorithm. In general, SGD finds a local minimum of a nonconvex objective function (Ge et al., 2015) but a global minimizer in some special situations (Raginsky et al., 2017; Wu et al., 2018).

Lemma 6 is a version of Theorems 2 and 4, leading to the desired asymptotic null distribution and power of the one-split test in this specific example.

**Lemma 6** *If  $m = o(n^{2\gamma})$  with  $\gamma = 1 - \omega$  for any  $\omega > 0$ , then the one-split test in (2) based on  $\hat{f}_n$  and  $\hat{g}_n$  from (10) satisfies:*

$$\begin{aligned} \lim_{n \rightarrow \infty} \mathbb{P}(P^{(1)} \leq \alpha | H_0) &= \alpha, & \lim_{n \rightarrow \infty} \mathbb{P}(\bar{P}^{(1)} \leq \alpha | H_0) &\leq \alpha, & \text{under } H_0, \\ \lim_{\delta \rightarrow \infty} \liminf_{n \rightarrow \infty} \pi_n(\delta) &= 1, & \lim_{\delta \rightarrow \infty} \liminf_{n \rightarrow \infty} \bar{\pi}_n(\delta) &= 1, & \text{under } H_a, \end{aligned}$$

As a remark, we note that Lemma 6 can be extended to a misspecified model situation, where  $f^* \notin \mathcal{H}$  but belongs to a larger space such as  $\mathcal{C}_d^\beta$ , the  $\beta$ -Hölder functional space. In such a situation, the approximation error of  $f^*$  by  $\mathcal{H}$  plays a role in the rate of convergence. Still, the rate in Assumption A can be obtained; for instance, the rate is  $n^{-\beta/(2\beta+d+5)}$  for a neural net with one hidden layer (McCaffrey and Gallant, 1994), and the rate is  $n^{-2\beta/(2\beta+d)}(\log n)$  for a two-layer neural net with the sigmoid activation function (Kohler and Krzyżak, 2005, 2016). Moreover, the numerical experiment for a misspecified model situation is illustrated in Section 6.3.

## 5. Sample splitting

The one-split and two-split tests require the sample splitting ratio  $\zeta$  to satisfy the requirement  $m = o(n^{2\gamma})$  to control the Type I error. In this section, we develop two computing schemes, namely “log-ratio” and “data-adaptive” tuning schemes, to estimate  $\zeta$  in addition to the perturbation size  $\rho$  for the one-split test.

### 5.1 Log-ratio sample splitting scheme

This subsection proposes a log-ratio splitting scheme to ensure automatically the requirement  $m = o(n^{2\gamma})$ . Specifically, given a sample size  $N \geq N_0$ , where  $N_0$  is the minimal sample size required for the hypothesis testing, the estimation and inference sizes  $n$  and  $m$  are obtained:

$$n = \lceil x_0 \rceil, \quad m = N - n, \quad \text{where } x_0 \text{ is a solution of } \left\{ x + \frac{N_0}{2 \log(N_0/2)} \log(x) = N \right\}. \quad (11)$$

	Total sample size ( $N$ )					
	2000	5000	10000	20000	50000	100000
Estimation sample size ( $n$ )	1000	3807	8688	18578	48439	98336
Inference sample size ( $m$ )	1000	1193	1312	1422	1561	1664

Table 1: Illustration of split sample sizes  $(n, m)$  using the log-ratio splitting formula (11) as the total sample size  $N$  increases from 2000 to 100000 while  $N_0 = 2000$  is fixed.

**Lemma 7** *The estimation and inference sample sizes  $(n, m)$ , determined by the log-ratio sample splitting formula (11), satisfies  $m = o(n^{2\gamma})$  for any  $\gamma > 0$  in Assumption A.*

## 5.2 Heuristic data-adaptive tuning scheme

The log-ratio formula in (11) is relatively conservative as the inference sample size  $m$  increases in the logarithm of the estimation sample size  $n$ . To further increase a test's power, we develop a heuristic data-adaptive tuning scheme as an alternative.

The data-adaptive tuning scheme selects  $(\zeta, \rho)$  by controlling the estimated Type I error on permuted inference samples. To proceed, we permute hypothesized features for an entire sample, that is, permuting  $\{\mathbf{X}_i, Y_i\}_{i=1}^N = \{\mathbf{X}_{i,S}, \mathbf{X}_{i,S^c}, Y_i\}_{i=1}^N$  to  $\{\tilde{\mathbf{X}}_i, \tilde{Y}_i\}_{i=1}^N = \{\mathbf{X}_{\pi(i),S}, \mathbf{X}_{i,S^c}, Y_i\}_{i=1}^N$ , where  $\pi$  is a permutation mapping. Note that the hypothesized features for this permuted sample are irrelevant to the prediction of the outcome; that is, the null hypothesis  $H_0$  is true.

Given a ratio value  $\zeta = m/N$ , we first split the entire sample into an estimation sample  $\{\mathbf{X}_i, Y_i\}_{i=1}^n$  and an inference sample  $\{\mathbf{X}_i, Y_i\}_{i=n+1}^{n+m}$ . Then, we permute the estimation sample to generate a permuted estimation sample  $\{\tilde{\mathbf{X}}_i, \tilde{Y}_i\}_{i=1}^n$ , which is used for fitting  $\hat{f}_n$  and  $\hat{g}_n$ . Then we permute the inference sample  $T$  times, denoted by  $\pi^{(t)}$ ;  $t = 1, \dots, T$ , to generate  $T$  permuted samples  $(\tilde{\mathbf{X}}_i^{(t)}, \tilde{Y}_i^{(t)})_{i=n+1}^N$ ;  $t = 1, \dots, T$ . Note that the Type I error of the one-split test is  $\text{Err}_1(\rho, \zeta) = \mathbb{P}(\Lambda_n^{(1)} \leq z_\alpha | H_0)$ . Then an estimated Type I error is computed as:

$$\widehat{\text{Err}}_1(\rho, \zeta) = T^{-1} \sum_{t=1}^T \mathbb{I}(\Lambda_n^{(1,t)} \leq z_\alpha), \quad (12)$$

where  $\Lambda_n^{(1,t)}$  is the test statistic  $\Lambda_n^{(1)}$  based on the permuted estimation and inference samples  $\{\tilde{\mathbf{X}}_i, \tilde{Y}_i\}_{i=1}^n$  and  $\{\tilde{\mathbf{X}}_i^{(t)}, \tilde{Y}_i^{(t)}\}_{i=n+1}^N$ .

The splitting ratio  $\zeta$  controls the trade-off between Type I error and statistical power. Specifically, a small  $\zeta$  value tends to yield biased estimators  $(\hat{f}_n, \hat{g}_n)$ , yielding an elevated Type I error exceeding the nominal level  $\alpha$ , yet could increase the power because of an enlarged inference sample. The perturbation size  $\rho$ , as mentioned early, controls the *bias-sd-ratio* to ensure the validity of the asymptotic null distribution.

For the one-split test, the data-adaptive scheme estimates  $(\zeta, \rho)$  as the smallest values in some candidate sets that controls an estimated Type I error. In the process of searching candidate sets  $\boldsymbol{\zeta}$  and  $\boldsymbol{\rho}$ , it stops once the termination criterion  $\widehat{\text{Err}}_1(\rho, \zeta) \leq \alpha$  is met, which intends to reduce the computational cost. In particular,

$$(\hat{\rho}, \hat{\zeta}) = \min_{\rho, \zeta} \{\rho \in \boldsymbol{\rho}, \zeta \in \boldsymbol{\zeta} : \widehat{\text{Err}}_1(\rho, \zeta) \leq \alpha\}, \quad (13)$$

where  $\alpha > 0$  is the nominal level,  $\widehat{\text{Err}}_1(\rho, \zeta)$  is the estimated Type I error computed via (12),  $\boldsymbol{\zeta}$  and  $\boldsymbol{\rho}$  represent sets of candidate  $\zeta$  and  $\rho$  values, for example,  $\boldsymbol{\zeta} = \{.2, .4, .6, .8\}$  and  $\boldsymbol{\rho} = \{.01, .05, .1, .5, 1.0\}$ .

Algorithm 1 summarizes the computational scheme of the one-split test. For the non-combining test in Algorithm 1, the data-adaptive scheme usually requires 2-3 times of training and evaluations since the loop for the splitting ratio usually terminates in one or two iterations. For the combined test, the data-adaptive scheme based on 5 random splits usually requires 7-8 times of training and evaluations. The running time for the proposed test is indicated in Tables 3 and 17.

---

**Algorithm 1:** One-split test for feature relevance to prediction

---

**Input** : Data:  $(\mathbf{x}_i, \mathbf{y}_i)_{i=1}^N$ ; Set of hypothesized features:  $\mathcal{S}$ ; Number of splitting:  $U$   
**Output**:  $p$ -value for testing (1)

```

1 Estimate  $(\hat{\rho}, \hat{\zeta})$  from (13) ;
2 for  $u = 1, \dots, U$  do
3   | Shuffle the data;
4   | Split the data into an estimation sample and an inference sample, where
      |  $m = \hat{\zeta}N$  and  $n = N - m$ ;
5   | Compute  $\Lambda_u^{(1)}$  from (2);
6   | Compute  $p$ -value  $P_u^{(1)} = \Phi(\Lambda_u^{(1)})$ 
7 end
8 if  $U > 1$  then                                     // combined one-split test
9   | Compute the combined  $p$ -value  $\bar{P}^{(1)}$  via (7) ;
10  | return  $p$ -value  $\bar{P}^{(1)}$ 
11 else                                                  // non-combined one-split test
12  | return  $p$ -value  $P_1^{(1)}$ 
13 end
```

---

## 6. Numerical examples

This section examines the proposed tests for their capability of controlling Type I error and power in both simulated and real examples. All tests are implemented in our Python library `dnn-inference` (<https://github.com/statmlben/dnn-inference>).

### 6.1 Numerical comparison with existing blackbox tests

This subsection presents a simple example to illustrate the differences between the proposed tests and other existing blackbox tests, including the holdout randomization test (HRT; (Tansey et al., 2018)), the leave-one-covariate-out test (LOCO; (Lei et al., 2018)), the permutation test (PT; (Breiman, 2001; Ojala and Garriga, 2010)), and the holdout permutation test (HPT; (Tansey et al., 2018)). For PT, we use the scheme of (Ojala and Garriga, 2010) to permute multiple hypothesized features  $\mathbf{X}_{\mathcal{S}}$ , on which we refit the model. Algorithm 2 summarizes the procedure for the permutation test. Note that we exclude CRT here due to its enormously expensive computing in refitting a model many times.

To alleviate the high computational cost of refitting, HPT uses data-splitting into a training sample and a test sample. Then it fits only one time on training data and performs the permutation test over the test sample with the trained model. On our content, we generate HPT in (Tansey et al., 2018) by simultaneously permuting multiple hypothesized features  $\mathbf{X}_{\mathcal{S}}$ .

One issue with the PT and HPT is that permutations of hypothesized features usually alter the dependence structure between  $\mathbf{X}_{\mathcal{S}}$  and  $\mathbf{X}_{\mathcal{S}^c}$ . As a result, the sampling distribution based on permuted samples may differ from the null distribution. For example, the simulated example in Appendix B.2 indicates that both HPT and PT lead to dramatically inflated Type I errors.

**Algorithm 2:** Permutation test for feature relevance to prediction.

**Input** : Data  $\mathcal{D} = (\mathbf{x}_i, \mathbf{y}_i)_{i=1}^N$ ; Set of hypothesized features:  $\mathcal{S}$ ; Number of permutations  $T$

**Output:**  $p$ -values for testing (1)

- 1 Compute the cross-validation score  $s_0$  on data  $\mathcal{D}$ .
- 2 **for**  $t = 1, \dots, T$  **do**
- 3     Generate  $\mathcal{D}_t$  by simultaneously permuting values of hypothesized features in  $H_0$ .
- 4     Compute the cross-validation score  $s_t$  based on data  $\mathcal{D}_t$
- 5 **end**
- 6 Compute  $p$ -value:

$$\hat{p} = \frac{|\{s_t \leq s_0 | t = 1, \dots, T\}| + 1}{T + 1}.$$

Test	Return	$H_0$	
One-split	$p$ -value	risk-invariance $R(f^*) = R_{\mathcal{S}}(g^*)$ ,	0.003
Two-split	$p$ -value	risk-invariance $R(f^*) = R_{\mathcal{S}}(g^*)$	0.018
HRT	$p$ -values for all feats	conditional indep $\mathbf{X}_j \perp \mathbf{Y}   \mathbf{X}_{-j}$	(0.840, 0.045, 0.064, 0.900, 0.158)
LOCO	$p$ -values for all feats	equal errors with/without feat $j$ for a given dataset	(0.132, 0.791, 0.180, 0.435, 0.342)
PT	$p$ -value	marginal indep $\mathbf{X}_{\mathcal{S}} \perp \mathbf{Y}$	0.010
HPT	$p$ -value	marginal indep $\mathbf{X}_{\mathcal{S}} \perp \mathbf{Y}$	0.001

Table 2: Returning values of the one-split, two-split and other existing blackbox tests. Here one-split, two-split, HRT, LOCO, PT, and HPT denote the proposed tests in Algorithms 1 and 3, the holdout randomization test (HRT; (Tansey et al., 2018)), the leave-one-covariate-out test (LOCO; (Lei et al., 2018)), permutation test (PT), and the holdout permutation test (HPT; (Tansey et al., 2018)). For the permutation test, the permutation size is 100.

In this section, we generate a random sample of size  $N = 1000$ . First,  $\mathbf{X} = (X_1, \dots, X_5)^\top$  follows a uniform distribution on  $[-1, 1]$  with a pairwise correlation  $\rho_{ij} = 0.5^{|i-j|}$ ;  $i, j = 1, \dots, 5$ . Second, the outcome  $Y$  is generated as  $Y = 0.02(X_1 + X_2 + X_3) + 0.05\epsilon$ , where  $\epsilon \sim N(0, 1)$ .

A simulation study is performed for the one-split and two-split tests, HRT, LOCO, and HPT. For HRT, we use the code of (Tansey et al., 2018) available at Github<sup>1</sup> with a default mixture density network with 2 components. For other methods, we fit a linear function based on stochastic gradient descent (SGD) with the same fitting parameters, that is, `epochs` is 100, `batch_size` is 32, and early stopping is used based on the mean squared error (MSE) with `validation_split` being 0.2 and `patience` being 10, where `patience` is the number of epochs until termination if no progress is made on the validation set. For HRT, LOCO, HPT and PT, an estimation and inference sample ratio is fixed as 0.8, and the data-adaptive scheme is used for the proposed tests.

The returning values are summarized in Table 2: the one-split and two-split tests return valid  $p$ -values for the hypothesis in (1) with  $\mathcal{S} = \{1, 2, 3\}$ , HRT and LOCO return  $p$ -

1. <https://github.com/tansey/hrt>

values for individual features with respect to conditional independence and error-invariance for a given dataset, respectively. PT and HPT provide  $p$ -values with respect to marginal independence. Therefore, the proposed tests are the only ones really targeting the specified null hypothesis in (1).

## 6.2 Simulations

We perform simulations in (9), where  $\mathbf{X} \sim N(\mathbf{0}, B\mathbf{\Sigma})$ ,  $\Sigma_{ij} = r^{|i-j|}$ ,  $r \in [0, 1]$ ,  $d$  is the dimension of the feature,  $r$  represents the correlation coefficient of features,  $B$  controls the magnitude of the features,  $(L, \varpi, \tau)$  denotes the depth, width, and the  $L_2$ -norm of the neural network in (9),  $\mathcal{S}_0 = \{1, \dots, |\mathcal{S}_0|\}$  is an index set of the true non-discriminative features, and  $\mathcal{S}$  is an index set of hypothesized features.

Now consider hypotheses,  $H_0 : R(f^*) - R_{\mathcal{S}}(g^*) = 0$  versus  $H_a : R(f^*) - R_{\mathcal{S}}(g^*) < 0$ . We examine four index sets of hypothesized features  $\mathcal{S}$ : (i)  $\mathcal{S} = \{1, \dots, |\mathcal{S}_0|\}$ , (ii)  $\mathcal{S} = \{\lfloor |\mathcal{S}_0|/2 \rfloor, \dots, \lfloor |\mathcal{S}_0|/2 \rfloor + |\mathcal{S}_0|\}$ , (iii)  $\mathcal{S} = \{\lfloor p/2 \rfloor, \dots, \lfloor p/2 \rfloor + |\mathcal{S}_0|\}$ , (iv)  $\mathcal{S} = \{p - |\mathcal{S}_0|, \dots, p\}$ . These four sets are illustrated in Figure 2. Note that  $\mathcal{S} \cup \mathcal{S}_0 = \mathcal{S}_0$  in (i), implying that it is for Type I error analysis, while  $\mathcal{S} \cup \mathcal{S}_0 \neq \mathcal{S}_0$  in (ii)-(iv), suggesting power analyses. From (ii) to (iv), the distance (or correlation) between the hypothesized features  $\mathcal{S}$  and those non-discriminative features in  $\mathcal{S}_0$  is increasing (or decreasing), thus the power is expected to go up. Six examples are considered for the four situations.

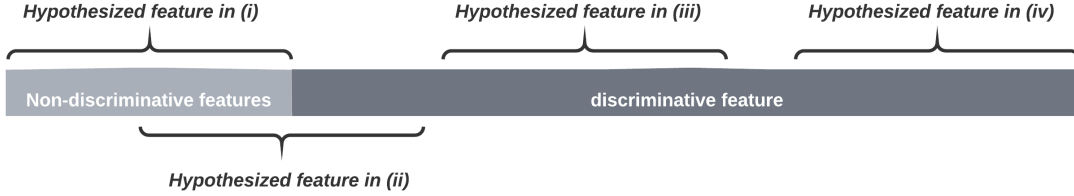


Figure 2: Illustration of four index sets of hypothesized features in simulations: (i) Type I error analysis, (ii)-(iv): Power analysis. Note that the impact of the hypothesized features  $\mathcal{S}$  on  $\mathcal{S}_0$  decreases while the power is expected to increase from (ii) to (iv).

**Example 1.** (*Impact of the sample size and tuning method*) This example (Table 3) concerns the performance of the proposed tests in relation to the sample size  $N$  based on *log-ratio* and *data-adaptive* tuning methods, where  $N$  ranges from 2000 to 10000,  $B = 0.4$ ,  $r = 0.25$ ,  $p = 100$ ,  $\varpi = 128$ ,  $\tau = 2$ ,  $L = 3$ ,  $|\mathcal{S}_0| = 5$ .

**Example 2.** (*Impact of the strength of features of interest*) This example (Table 4) concerns the performance of the proposed tests with respect to the magnitude of hypothesized features  $B$ , where  $B = 0.2, 0.4, 0.6$ ,  $N = 6000$ ,  $p = 100$ ,  $r = 0.25$ ,  $\varpi = 128$ ,  $\tau = 2$ ,  $L = 3$ , and  $|\mathcal{S}_0| = 5$ .

**Example 3.** (*Impact of the depth and width of a neural network*) This example (Table 17) concerns the performance of the proposed tests in terms of the width  $\varpi$  and depth  $L$  of a neural network, where  $N = 6000$ ,  $L = 2, 3, 4$ ,  $\varpi = 32, 64, 128$ ,  $B = 0.4$ ,  $r = 0.25$ ,  $p = 100$ ,  $\tau = 2$ ,  $L = 3$ , and  $|\mathcal{S}_0| = 5$ .

**Example 4.** (*Impact of the number of hypothesized features*) This example (Table 5) concerns the proposed tests with respect to the number of hypothesized features  $|\mathcal{S}_0|$ , where  $|\mathcal{S}_0| = 5, 10, 15$ ,  $N = 6000$ ,  $B = 0.4$ ,  $p = 100$ ,  $\varpi = 128$ ,  $r = 0.25$ ,  $\tau = 2$ , and  $L = 3$ .

**Example 5.** (*Impact of feature correlations*) This example (Table 6) concerns the proposed tests in terms of the feature correlation  $r$ , where  $r = 0.00, 0.25, 0.50$ ,  $N = 6000$ ,  $B = 0.4$ ,  $p = 100$ ,  $\varpi = 128$ ,  $\tau = 2$ ,  $L = 3$ , and  $|\mathcal{S}_0| = 5$ .

**Example 6.** (*Impact of different modes of combining p-values*) This example (Table 18) concerns the combined tests with different ways of combining p-values, including the Hommel, the Bonferroni, the first quantile, the median, the Cauchy, and the harmonic methods. The power and Type I errors of these tests will be examined in two simulated examples: (1)  $N = 6000$ ,  $\rho = 0.25$ ,  $B = 0.2$ ,  $L = 3$ ,  $\varpi = 128$ ; (2)  $N = 6000$ ,  $\rho = 0.25$ ,  $B = 0.4$ ,  $L = 4$ ,  $\varpi = 32$ .

Splitting method	Test	Sample size	Type I error	Power	Time (Second)
<i>Log-ratio</i>	One-split	2000	0.004	(0.22, 0.88, 0.92)	8.1(0.4)
		6000	0.004	(0.42, 1.00, 1.00)	9.6(0.6)
		10000	0.010	(0.45, 1.00, 1.00)	11.7(0.4)
	Two-split	2000	0.026	(0.11, 0.34, 0.35)	8.4(0.4)
		6000	0.036	(0.09, 0.45, 0.42)	9.7(0.5)
		10000	0.034	(0.16, 0.46, 0.43)	11.4(0.2)
	Comb. one-split	2000	0.016	(0.24, 0.95, 0.95)	42.1(1.6)
		6000	0.012	(0.51, 1.00, 1.00)	45.6(1.3)
		10000	0.010	(0.67, 1.00, 1.00)	56.3(0.8)
	Comb. two-split	2000	0.018	(0.10, 0.30, 0.32)	40.8(1.6)
		6000	0.024	(0.09, 0.49, 0.47)	45.5(1.2)
		10000	0.018	(0.08, 0.41, 0.42)	56.5(1.1)
<i>Data-adaptive</i>	One-split	2000	0.043	(0.25, 0.79, 0.85)	15.2(0.1)
		6000	0.050	(0.61, 0.99, 1.00)	41.2(0.3)
		10000	0.049	(0.89, 1.00, 1.00)	66.0(0.4)
	Two-split	2000	0.050	(0.11, 0.26, 0.31)	14.0(0.1)
		6000	0.035	(0.18, 0.51, 0.58)	37.0(0.2)
		10000	0.040	(0.19, 0.77, 0.75)	61.6(0.4)
	Comb. one-split	2000	0.034	(0.26, 1.00, 0.95)	37.9(0.1)
		6000	0.046	(0.86, 1.00, 1.00)	68.3(0.3)
		10000	0.045	(1.00, 1.00, 1.00)	107.2(0.7)
	Comb. two-split	2000	0.015	(0.09, 0.26, 0.29)	38.0(0.1)
		6000	0.030	(0.10, 0.70, 0.65)	76.3(0.5)
		10000	0.014	(0.13, 0.93, 0.92)	110.3(0.5)

Table 3: Empirical Type I errors and powers of the one-split and two-split tests, their combined tests in Example 1 at a nominal level  $\alpha = 0.05$ .

For a test’s size and power, we compute the proportions of its rejecting  $H_0$  out of 1000 simulations under  $H_0$  and out of 100 simulations under  $H_a$ , respectively.

When implementing the “log-ratio” splitting scheme,  $(n, m)$  is determined by (11) with  $N_0 = 1000$ , and  $\rho = 0.01$ ; for the data-adaptive scheme, the grids of  $\zeta$  are set as  $\{0.2, 0.4, 0.6, 0.8\}$ . Moreover, the grids for searching the optimal perturbation size are  $\{0.01, 0.05, 0.1, 0.5, 1.0\}$ . The hyper-parameters of a neural network are the same for all tests; that is, `epochs` is 100, `batch_size` is 512, and early stopping is used based on the mean squared error (MSE) with `validation_split` being 0.2 and `patience` being 50, where



Test	$B$	Type I error	Power
One-split	0.2	0.057	(0.24, 0.68, 0.78)
	0.4	0.050	(0.61, 0.99, 1.00)
	0.6	0.057	(0.97, 1.00, 1.00)
Two-split	0.2	0.049	(0.06, 0.12, 0.14)
	0.4	0.035	(0.18, 0.51, 0.58)
	0.6	0.041	(0.37, 0.97, 0.98)
Comb. one-split	0.2	0.027	(0.27, 0.93, 0.93)
	0.4	0.046	(0.86, 1.00, 1.00)
	0.6	0.033	(1.00, 1.00, 1.00)
Comb. two-split	0.2	0.019	(0.00, 0.00, 0.03)
	0.4	0.030	(0.10, 0.70, 0.65)
	0.6	0.012	(0.45, 1.00, 1.00)

Table 4: Empirical Type I errors and powers of the one-split and two-split tests, and their combined tests in Example 2 at a nominal level  $\alpha = 0.05$ . The data-adaptive tuning scheme is applied.

Test	$ S_0 $	Type I error	Power
One-split	3	0.047	(0.28, 0.95, 0.96)
	5	0.050	(0.61, 0.99, 1.00)
	10	0.037	(1.00, 1.00, 1.00)
Two-split	3	0.052	(0.09, 0.19, 0.31)
	5	0.035	(0.18, 0.51, 0.58)
	10	0.042	(0.59, 0.95, 0.98)
Comb. one-split	3	0.035	(0.24, 1.00, 1.00)
	5	0.046	(0.86, 1.00, 1.00)
	10	0.019	(1.00, 1.00, 1.00)
Comb. two-split	3	0.020	(0.05, 0.20, 0.19)
	5	0.030	(0.10, 0.70, 0.65)
	10	0.013	(0.72, 1.00, 1.00)

Table 5: Type I errors and powers of the one-split and two-split tests and their combined tests in Example 4 at a nominal level  $\alpha = 0.05$ . The data-adaptive tuning scheme is applied.

**patience** is the number of epochs until termination if no progress is made on the validation set. For combined tests, the number of repeated random splitting is set as 5.

**Power and empirical size of the one-split, two-split, and combined tests.** As indicated in Tables 3 - 6, the one-split and two-split tests perform well in Examples 1-5 with respect to controlling Type I error and yielding high power. In particular, Type I errors are close to the nominal level  $\alpha = 0.05$ , whereas the power functions increase to 1 as the sample size  $N$  increases. As expected, the one-split test dominates the two-split test in terms of statistical power, which agrees with our power analysis in Theorems 4 and 10. The combined one-split and two-split tests consistently improve over their one-split and two-

Test	$r$	Type I error	Power
One-split	0.00	0.044	(0.55, 0.98, 0.96)
	0.25	0.050	(0.61, 0.99, 1.00)
	0.50	0.052	(0.89, 1.00, 1.00)
Two-split	0.00	0.040	(0.09, 0.32, 0.35)
	0.25	0.035	(0.18, 0.51, 0.58)
	0.50	0.039	(0.09, 0.80, 0.79)
Comb. one-split	0.00	0.029	(0.64, 1.00, 1.00)
	0.25	0.046	(0.86, 1.00, 1.00)
	0.50	0.033	(0.98, 1.00, 1.00)
Comb. two-split	0.00	0.018	(0.04, 0.38, 0.31)
	0.25	0.030	(0.10, 0.70, 0.65)
	0.50	0.022	(0.09, 0.95, 0.98)

Table 6: Empirical Type I errors and powers of the one-split and two-split tests and their combined tests in Example 5 at a nominal level  $\alpha = 0.05$ . The data-adaptive tuning scheme is applied.

split tests in terms of power while controlling the Type I error. Specifically, the combined one-split and two-split tests tend to have higher power but slightly lower empirical Type I error.

**Runtime.** The combined tests may double the runtime of their non-combined counterparts based on the data-adaptive tuning scheme. This result suggests that the one-split, two-split, and their combined tests are practically feasible for inference subject to computational constraints as in the case of applying deep neural networks to large data.

**Combining p-values.** As suggested by Table 18, the Hommel combining method controls the Type I error while having reasonably good power. The Bonferroni and Cauchy methods have an issue of failing to control Type I error, whereas the 1<sup>st</sup>-Quantile, median, and harmonic methods lose power in the first case of Example 6.

We summarize the advantages of the different tests and the combining/tuning methods in Table 7.

		Advantage	Evidence
Test	One-split	<i>More powerful</i>	Tables 3, 4, 5
	Two-split	<i>No need to perturb data</i>	(14)
Combine	Comb.	<i>More powerful</i>	Tables 3, 4, 5
	Non-comb.	<i>Less computation time</i>	Table 3
Ratio	Data-adaptive	<i>More powerful</i>	Tables 3, 4, 5
	Log-ratio	<i>No need to tune the ratio, and less computation time</i>	Lemma 7, Table 3

Table 7: Advantage for different tests, combining, and tuning methods.

### 6.3 Simulation for model misspecification

This subsection examines performance for the proposed tests in situation that the true regression function  $f^*$  belongs to a bigger class than a neural network class  $\mathcal{H}$ . Toward this end, we simulate random samples  $(\mathbf{X}_i, Y_i)_{i=1}^N$  as follows. First, we simulate  $\mathbf{X}_i$  from  $N(\mathbf{0}, \mathbf{I}_d)$  with  $d = 10$ . Second, we generate  $Y_i$ :

$$Y_i = 0.1X_{i6} + 0.2X_{i7}^2 + 0.3X_{i8}^3 + 0.4X_{i9}X_{i10} + 0.3\epsilon,$$

where  $\epsilon \sim N(0, 1)$ . Now consider the null hypothesis in (1) to determine if  $\mathbf{X}_{\mathcal{S}}$  is functionally relevant to the prediction of  $Y$  with the true null  $H_0$  and alternative  $H_a$  hypotheses in three cases: (i)  $\mathcal{S} = \{1, \dots, 5\}$ , (ii)  $\mathcal{S} = \{3, \dots, 7\}$ , (iii)  $\mathcal{S} = \{6, 7, 8\}$ , where the sample size  $N$  is 1000, 2000, 6000. Note that (i) is for Type I error analysis and (ii)-(iv) are for power analysis.

As indicated in Table 8, the proposed tests control the Type I errors for all different sample sizes, and the power increases as the sample size becoming larger. The numerical results also confirm the theoretical analysis in Section 4.

Test	Sample size	Type I error	Power
One-split	1000	0.000	(0.11, 1.00)
	2000	0.000	(0.56, 1.00)
	6000	0.002	(0.97, 1.00)
Two-split	1000	0.000	(0.02, 0.77)
	2000	0.001	(0.33, 0.95)
	6000	0.001	(0.94, 1.00)
Comb. one-split	1000	0.028	(0.15, 1.00)
	2000	0.000	(0.79, 1.00)
	6000	0.001	(1.00, 1.00)
Comb. two-split	1000	0.000	(0.02, 0.82)
	2000	0.002	(0.33, 1.00)
	6000	0.002	(1.00, 1.00)

Table 8: Empirical Type I errors and powers of the one-split, two-split tests, and their combined tests in misspecified situation in Section 6.3 at a nominal level  $\alpha = 0.05$ . The data-adaptive scheme is applied to determine the splitting ratio and perturbation size.

### 6.4 One-split test and perturbation

Consider a regression model in (9), where  $\mathcal{S}_0 = \{1, 2, 3\}$ ,  $\mathbf{X} \sim N(\mathbf{0}, B\mathbf{\Sigma})$ ,  $\Sigma_{ij} = r^{|i-j|}$ ,  $r \in [0, 1)$ . Additionally, we set  $\Sigma_{1j} = \Sigma_{j1} = .1$ ;  $j = 1, \dots, p$ , and  $\Sigma_{ij} = 0$ , if  $i, j \neq 1$  and  $i \neq j$ . In this case, let  $\mathcal{S} = \mathcal{S}_0$ , then  $H_0$  is true in the population level. Furthermore, only partial features are observed in a sample  $(\mathbf{x}_i^{(N)}, y_i^{(N)})_{i=1}^N$ , where  $\mathbf{x}_i^{(N)} = (\mathbf{x}_{i1}, \dots, \mathbf{x}_{id_N})^\top$  and  $y_i^{(N)} = f^*(\tilde{\mathbf{x}}_i^{(N)}) + \epsilon_i$ , where  $\epsilon_i \sim N(0, 1)$ ,  $d_N \leq d$  is the number of observed features in the finite sample situation and  $d_N \rightarrow d$  as  $N \rightarrow \infty$ , and  $\tilde{\mathbf{x}}_i^{(N)} = (\mathbf{x}_{i1}, \dots, \mathbf{x}_{id_N}, 0, \dots, 0)^\top$  is a  $d$ -dimensional vector.

Given a random sample  $(\mathbf{x}_i^{(N)}, y_i^{(N)})_{i=1}^N$ , we set  $d = 100$ ,  $d_N = \lfloor d(1 - \frac{1}{\log(N)}) \rfloor$ , and  $N = 2000, 6000, 10000$ . For implementation, we set  $\zeta = 0.2$  for the one-split and two-split tests and  $\rho = 1.0$  for the one-split test. The fitting parameters of a neural net remain the same as in Section 6.2. Then, the Type I error for  $\mathcal{S} = \mathcal{S}_0$  based on the proposed one-split test without perturbation is reported in Table 9.

Test	$N = 2000$	$N = 6000$	$N = 10000$
One-split without perturbation	0.083	0.109	0.193
One-split with perturbation	0.057	0.053	0.061
Two-split	0.048	0.051	0.047

Table 9: Type I errors of the one-split tests with and without perturbation and the two-split test in Section 6.4 at a nominal level  $\alpha = 0.05$ .

As indicated in Table 9, the two-split test and the one-split with perturbation approximately control Type I errors across all situations, whereas the one-split test without perturbation has inflated Type I errors significantly exceeding the nominal level  $\alpha = 0.05$ .

### 6.5 MNIST handwritten digits

This subsection applies the proposed test to the MNIST handwritten digits dataset<sup>2</sup> (LeCun et al., 1998). In particular, we extract 14,251 images from the dataset with labels ‘7’ and ‘9’ to discriminate between these two digits. Our primary goal is to test certain image features differentiating digit ‘7’ from digit ‘9’, where a marked region of an image specifies hypothesized features.

To proceed, we first produce a masked image by replacing pixels of a hypothesized region of an original image as zero. Then, we train two convolution neural nets (CNNs) respectively based on the original and masked MNIST datasets, each of which uses the default net provided by Keras targeted MNIST dataset<sup>3</sup>. Third, we perform a hypothesis test with a null hypothesis  $H_0$  that a marked region of interest is non-discriminative between digits 7 and 9 versus its alternative hypothesis  $H_a$  that it is not. The fitting parameters of a neural network are as follows: `epochs` is 100, `batch_size` is 512, and early stopping is used based on the misclassification error with `validation_split` being 0.2 and `patience` being 15. The number of repeated random splitting is set as 3 for combined tests. Finally, we apply the one-split test, the two-split tests, and their combined tests based on the data-adaptive tuning scheme with a significance level of  $\alpha = 0.05$ . More details are summarized in Table 10.

In this application, we consider three different types of masked regions, as displayed in Figure 3. In particular,

- Case 1.* A masked region is (19 : 28, 13 : 20), which indicates that  $H_0$  is true.
- Case 2.* A masked region is (21 : 28, 4 : 13), which indicates that  $H_0$  is true.
- Case 3.* A masked region is (7 : 16, 9 : 16), which indicates that  $H_a$  is true.

2. <http://yann.lecun.com/exdb/mnist/>

3. [https://keras.io/examples/mnist\\_cnn/](https://keras.io/examples/mnist_cnn/)

#Samples	Image dim	Dim of testing region	#Parameters
14,251	(28, 28)	(9, 7)	1,198,850

Table 10: Summary of MNIST dataset, the hypothesized region, and CNN. Here ‘#Samples’ indicates the number of samples in MNIST dataset, ‘Image dim’ is the dimension of an image, ‘Dim of testing region’ denotes the dimension of the hypothesized region, and ‘#Parameter’ is the number of parameters in the MNIST CNN.



Figure 3: Three cases for differentiating digits 7 and 9: Case 1 (first column)–Case 3 (third column), where The masked regions of interest are (19 : 28, 13 : 20), (21 : 28, 4 : 13), and (7 : 16, 9 : 16), respectively corresponding to the null hypotheses are true, true, and false.

We apply the one-split test, the two-split test, and their combined tests, with adaptive sampling splitting. Moreover, we compare these tests to the permutation test of the permutation size 100.

Test	$p$ -values (case 1, case 2, case 3)	Time(Second)
One-split	(0.174, 0.329, 0.000)	4289
Two-split	(0.959, 0.569, 0.000)	4772
Comb. one-split	(0.385, 1.000, 0.000)	11404
Comb. two-split	(0.544, 0.192, 0.000)	13060

Table 11: P-values and runtimes of the one-split and two-split tests, their combined tests, and the permutation test in the MNIST benchmark example at a nominal level  $\alpha = 0.05$ .

As suggested by Table 11, the one-split, two-split, and their combined tests all do not reject  $H_0$  at  $\alpha = 0.05$  when  $H_0$  is true in Cases 1-2, but all reject  $H_0$  in Case 3 when it is false. Overall, the test results confirm our intuition that the image features defined by the

marked regions in Cases 1 and 2 are visually indistinguishable for digits 7 and 9, whereas that in Case 3 is visually discriminative, as illustrated in Figure 3.

## 6.6 Chest X-rays for pneumonia diagnosis

This subsection illustrates the application of the proposed tests to chest X-ray images in a pneumonia diagnosis dataset<sup>4</sup> (Kermany et al., 2018). This dataset consists of 5,863 X-ray images, each labeled as “Pneumonia” or “Normal.” For quality-control all the images were preprocessed by removing low-quality or unreadable scans. Then each image was diagnosed and graded by two expert physicians before training. Finally, a third expert examined an evaluation set to guard against grading errors.

To proceed, we crop an image to produce a version of the image that focuses on the lung fields, based on DeepXR<sup>5</sup>. Then, we use a square cropping region to retain important areas containing parenchymal anatomy (pleural spaces) and retrocardiac anatomy (left lower pulmonary lobe). The detailed information for the preprocessed dataset is summarized in Table 12.

Next, we produce a masked image by setting the pixels of a hypothesized region to be zero. Then, we train two convolution neural nets (CNNs) respectively on the original and masked chest X-ray images, each of which uses a CNN for binary classification as suggested in a Kaggle notebook<sup>6</sup>. The fitting parameters for CNN are as follows: `epochs` is 50, `batch_size` is 16, and early termination involves the misclassification error with `validation_split` being 0.2 and `patience` being 10. The number of repeated random splitting is set as 5 for the combined tests. Finally, we apply the one-split test, two-split test, and their combined tests based on the data-adaptive tuning scheme at a significance level of  $\alpha = 0.05$ . More details are summarized in Table 12.

#Samples	Image dim	Dim of test region	#Parameters
5,863	(256, 256)	(150, 90), (150, 50), (150, 90)	7,882,274

Table 12: Summary for the hypothesis testing with the chest X-ray dataset. Here ‘#Samples’ indicates the number of samples in the chest X-ray dataset, ‘Image dim’ is the dimension of images, ‘Dim of testing region’ denotes the dimension of the hypothesized region, and ‘#Parameter’ is the number of parameters in the CNN.

Similarly, we also consider three different types of masked regions, as displayed in Figure 4. In particular,

- Case 1.* A masked region is (50 : 200, 20 : 110), for which  $H_0$  is likely to be false.
- Case 2.* A masked region is (50 : 200, 100 : 150), for which  $H_0$  is likely to be true.
- Case 3.* A masked region is (50 : 200, 150 : 240), for which  $H_0$  is likely to be false.

As suggested by Table 13, all tests fail to reject  $H_0$  at  $\alpha = 0.05$  in Case 2 when  $H_0$  is likely to be true. For Cases 1 and 3, only the one-split test rejects both the  $H_0$ , but other tests fail to do so when  $H_0$  is likely to be false. In agreement with the earlier results, the

4. <https://www.kaggle.com/paultimothymooney/chest-xray-pneumonia>

5. <https://github.com/IVPLatNU/DeepCovidXR>

6. <https://www.kaggle.com/sanwal092/intro-to-cnn-using-keras-to-predict-pneumonia>

Test	$p$ -values (case 1, case 2, case 3)	Time(Second)
One-split	(0.026, 0.995, 0.021)	15242
Two-split	(0.212, 0.561, 0.065)	14020
Comb. one-split	(0.041, 0.635, 0.075)	64416
Comb. two-split	(0.053, 0.754, 0.084)	64761

Table 13: P-values and runtimes of the one-split and two-split tests, and their combined tests in the chest X-ray dataset at a nominal level  $\alpha = 0.05$ .

one-split test seems more powerful to detect a discriminative region. Overall, the results confirm our visual impression that the two hypothesized regions in Cases 1 and 3 are visually distinguishable between normal and pneumonia subjects, as illustrated in Figure 4.

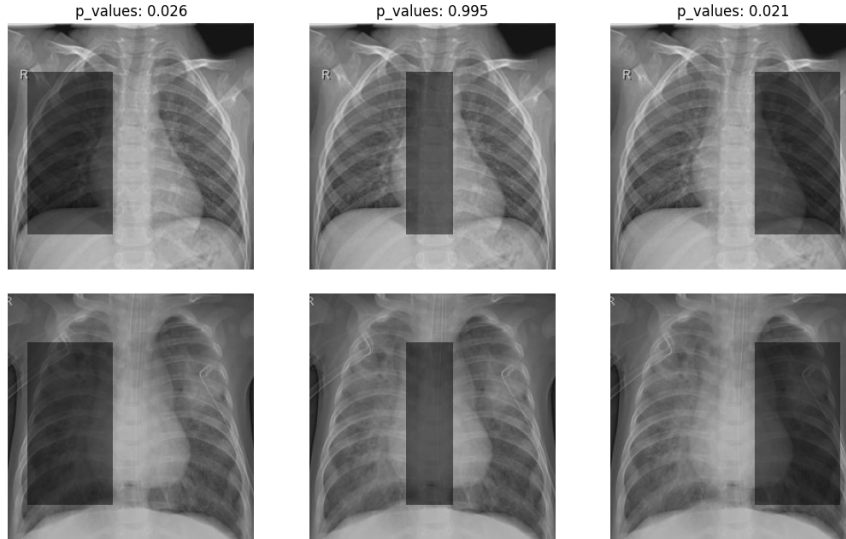


Figure 4: Three cases for “Normal” (first row) versus “Pneumonia” (second row) X-ray images. Marked regions for discriminating normal from pneumonia subjects are corresponding to Cases 1-3 (first to third columns), and the corresponding null hypotheses are likely to be false, true, and false.

## Acknowledgments

We thank the reviewers and the Editor for many helpful and constructive comments. We would like to acknowledge support for this project from NSF grants DMS-1712564, DMS-1721216 and DMS-1952539, and NIH grants 1R01GM126002 and R01HL105397.

## Appendix A. Two-split test

To treat the high *bias-sd-ratio* issue as described in Section 2, we propose an alternative of the one-split test by further splitting an inference sample into two equal subsamples yet the perturbation is not required. For simplicity, we assume  $m$  is an even number.

### A.1. Two-split test

Given  $(\hat{f}_n, \hat{g}_n)$ , we evaluate them based on these two independent subsamples to yield our two-split test statistic:

$$\Lambda_n^{(2)} = \frac{\sum_{j=1}^{m/2} \Delta_{n,j}^{(2)}}{\sqrt{\frac{m}{2} \hat{\sigma}_n^{(2)}}}, \quad \Delta_{n,j}^{(2)} = l(\hat{f}_n(\mathbf{X}_{n+j}), \mathbf{Y}_{n+j}) - l(\hat{g}_n(\mathbf{Z}_{n+m+j}), \mathbf{Y}_{n+m+j}), \quad (14)$$

where  $\hat{\sigma}_n^{(2)}$  is the sample standard deviation of  $\{\Delta_{n,j}^{(2)}\}_{j=1}^{m/2}$  given  $\hat{f}_n$  and  $\hat{g}_n$ . In this fashion, perturbation is no longer required.

Similarly, the two-split test proceeds as the one-split test except that its  $p$ -value is computed as  $P^{(2)} = \Phi(\Lambda_n^{(2)})$  based on Theorem 8.

To derive the asymptotic null distribution of  $\Lambda_n^{(2)}$ , we make the parallel assumptions B' and C'.

**Assumption B'** (Lyapounov condition for  $\Lambda_n^{(2)}$ ). Assume that

$$m^{-\mu} \mathbb{E}(|\Delta_{n,1}^{(2)}|^{2(1+\mu)} | \mathcal{E}_n) \xrightarrow{p} 0, \quad \text{as } n \rightarrow \infty$$

for some constant  $\mu > 0$ , where  $\Delta_{n,1}^{(2)}$  is defined in (14) and  $\xrightarrow{p}$  denotes convergence in probability.

**Assumption C'** (Variation estimation) Assume that  $\text{Var}(\Delta_{n,1}^{(2)} | \mathcal{E}_n) \xrightarrow{p} (\sigma^{(2)})^2$  as  $n \rightarrow \infty$ .

Under some mild assumptions,  $(\sigma^{(2)})^2 = \text{Var}(l(f^*(\mathbf{X}), \mathbf{Y})) + \text{Var}(l(g^*(\mathbf{Z}(\mathbf{X})), \mathbf{Y})) > 0$ , c.f., Lemma 6.

**Theorem 8 (Asymptotic null distribution)** *In addition to Assumptions A, B', and C', if  $m = o(n^{2\gamma})$ , then under  $H_0$ ,*

$$\Lambda_n^{(2)} \xrightarrow{d} N(0, 1), \quad \text{as } n \rightarrow \infty. \quad (15)$$

Furthermore, the  $p$ -value  $\bar{P}^{(2)}$  for the combined two-split test can be defined exactly as in (7).

**Theorem 9 (Type I error for the combined two-split test)** *Suppose that Assumption A and B'-C' are satisfied for the two-split test (14), if  $m = o(n^{2\gamma})$ , then under  $H_0$ , for any  $0 < \alpha < 1$  and any  $U \geq 2$ ,*

$$\lim_{n \rightarrow \infty} \mathbb{P}(\bar{P}^{(2)} \leq \alpha | H_0) \leq \alpha,$$

where  $\bar{P}^{(2)}$  is defined as the  $q$ -order test or the Hommel's test in (7) based on  $(P_1^{(2)}, \dots, P_U^{(2)})$ .



### A.2. Power analysis for two-split tests

This section performs power analysis of the two-split test in (14). Consider an alternative hypothesis  $H_a : R(f^*) - R_S(g^*) = -m^{-1/2}\delta < 0$  for  $\delta > 0$ . The power functions of the two-split test in (14) and its combined tests (7) can be written as

$$\pi_n^{(2)}(\delta) = \mathbb{P}(P^{(2)} \leq \alpha | H_a), \quad \bar{\pi}_n^{(2)}(\delta) = \mathbb{P}(\bar{P}^{(2)} \leq \alpha | H_a),$$

where  $\mathbb{P}(\cdot | H_a)$  denotes the probability under  $H_a$  and  $\alpha > 0$  is the nominal level.

Theorems 10 and 11 suggest that the power functions of the two-split test and its combined test tend to one as  $\delta \rightarrow \infty$ .

**Theorem 10 (Power of the two-split test)** *Under Assumption A,  $B'$  and  $C'$ , if  $m = o(n^{2\gamma})$ , then we have*

$$\lim_{n \rightarrow \infty} \inf \pi_n^{(2)}(\delta) = \Phi\left(\frac{\delta}{\sqrt{2\sigma^{(2)}}} - z_\alpha\right), \quad \text{and} \quad \lim_{\delta \rightarrow \infty} \liminf_{n \rightarrow \infty} \pi_n^{(2)}(\delta) = 1, \quad (16)$$

where  $z_\alpha = \Phi^{-1}(1 - \alpha)$  is the  $100(1 - \alpha)$ th percentile of the standard normal distribution.

**Theorem 11 (Power of the combined two-split test)** *Under Assumption A,  $B'$  and  $C'$ ,  $m = o(n^{2\gamma})$ , then for  $\bar{P}^{(2)}$  defined as the  $q$ -order combined test in (7), we have*

$$\lim_{n \rightarrow \infty} \inf \bar{\pi}_n^{(2)}(\delta) \geq 1 - \min\left(\frac{U}{\alpha q} \Gamma, 1\right), \quad \lim_{\delta \rightarrow \infty} \liminf_{n \rightarrow \infty} \bar{\pi}_n^{(2)}(\delta) = 1,$$

and for  $\bar{P}^{(2)}$  defined as the Hommel combined test (7), we have

$$\lim_{n \rightarrow \infty} \inf \bar{\pi}_n^{(2)}(\delta) \geq 1 - \min\left\{\frac{CU}{\alpha q} \Gamma, 1; q = 1, \dots, U\right\}, \quad \lim_{\delta \rightarrow \infty} \liminf_{n \rightarrow \infty} \bar{\pi}_n^{(2)}(\delta) = 1,$$

where  $\Gamma = \Phi\left(-\frac{\delta}{2\sigma^{(l)}}\right) + \sqrt{\frac{q-1}{U-q+1}}\left(\Phi\left(\frac{\delta}{2\sigma^{(l)}}\right) - \Phi^2\left(\frac{\delta}{2\sigma}\right) - 2T\left(-\frac{\delta}{2\sigma^{(l)}}, \frac{\sqrt{3}}{3}\right)\right)^{1/2}$ , and  $T(h, a) = (2\pi)^{-1} \int_0^a \frac{\exp(-h^2(1+x^2)/2)}{x^2+1} dx$  is Owen's  $T$  function (Owen, 1956), and

### A.3. Data-adaptive sample splitting for the two-split test

This section develops a computing scheme to determine the sample splitting ratio or  $\zeta$  to achieve our objective of controlling Type I error in a finite-sample situation.

As in Section 5 for the one-split test, Type I error of the two-split test is  $\text{Err}_2(\rho, \zeta) = \mathbb{P}(\Lambda_n^{(2)} \leq z_\alpha | H_0)$ , which is a function of splitting ratio  $\zeta$ :

$$\widehat{\text{Err}}_2(\zeta) = T^{-1} \sum_{t=1}^T \mathbb{I}(\Lambda_n^{(2,t)} \leq z_\alpha), \quad (17)$$

where  $\Lambda_n^{(l,t)}$ ;  $l = 1, 2$ , computed based on the permuted estimation sample  $\{\tilde{\mathbf{X}}_j^{(t)}, \tilde{Y}_j^{(t)}\}_{j=1}^n$  and the permuted inference sample  $\{\tilde{\mathbf{X}}_j^{(t)}, \tilde{Y}_j^{(t)}\}_{i=n+1}^N$ ;  $t = 1, \dots, T$ .

Moreover, data-adaptive is also applicable to the two-split test:

$$\hat{\zeta} = \min\{\zeta \in \zeta : \widehat{\text{Err}}_2(\zeta) \leq \alpha\}, \quad (18)$$

where  $\widehat{\text{Err}}_2(\zeta)$  is computed via (17). Furthermore,  $\zeta$  for the combined tests are estimated via (7), in which  $P^{(2)}$  is replaced by  $\bar{P}^{(2)}$  based on permuted sample. The computational scheme of the proposed two-split tests is summarized in Algorithm 3.

**Algorithm 3:** Two-split test for feature relevance to prediction

---

**Input** : Data:  $(\mathbf{x}_i, \mathbf{y}_i)_{i=1}^N$ ; Set of hypothesized features:  $\mathcal{S}$ ; Number of splitting:  $U$   
**Output**:  $p$ -value for the test (1)

```

1 Estimate  $\hat{\zeta}$  from (18) ;
2 for  $u = 1, \dots, U$  do
3   | Shuffle data;
4   | Split data into an estimation sample and an inference sample, where  $m = \hat{\zeta}N$ 
   |   and  $n = N - m$ ;
5   | Compute  $\Lambda_u^{(2)}$  from (2);
6   | Compute  $p$ -value  $P_u^{(2)} = \Phi(\Lambda_u^{(2)})$ 
7 end
8 if  $U > 1$  then                                     // combined two-split test
9   | Compute the combined  $p$ -value  $\bar{P}^{(2)}$  via (7) ;
10  | return  $p$ -value  $\bar{P}^{(2)}$ 
11 else                                                  // non-combined two-split test
12  | return  $p$ -value  $P_1^{(2)}$ 
13 end

```

---

**Appendix B. Additional numerical examples****B.1. Comparison with the likelihood ratio test for a non-blackbox learner**

This subsection compares the proposed tests with the likelihood ratio test (LRT) for a logistic regression, although the former is designed for a blackbox learner. In simulations, we generate a random sample  $(\mathbf{X}_i, Y_i)_{i=1}^N$  as follows. First, we generate a feature vector  $\mathbf{X}$  and the regression parameter vector  $\boldsymbol{\theta}$  from  $N(\mathbf{0}, \mathbf{I}_d)$ . Second, we generate a binary response  $Y$  as  $Y = \text{Sign}(\boldsymbol{\theta}^\top \mathbf{Z} + .1\epsilon)$  with  $\mathbf{Z}_{1:10} = \mathbf{0}$  and  $\mathbf{Z}_{11:100} = \mathbf{X}_{11:100}$ . Now consider a hypothesis test in (1) to determine if  $\mathbf{X}_{\mathcal{S}}$  is functionally relevant to the prediction of  $\mathbf{Y}$ , consider null  $H_0$  and alternative  $H_a$  hypotheses in three cases: (i)  $\mathcal{S} = \{1, \dots, 10\}$ , (ii)  $\mathcal{S} = \{5, \dots, 15\}$ , (iii)  $\mathcal{S} = \{10, \dots, 15\}$ , where the sample size  $N$  is 500, 800, 1000 and  $d = 100$ .

For implementation, we fit a logistic regression model with sample  $(\mathbf{X}_i, Y_i)_{i=1}^N$  via stochastic gradient descent with a learning rate 0.05 for LRT based on the Github repo<sup>7</sup>. For the proposed tests, we use the same fitting and splitting parameters for data-adaptive scheme as in Section 6.2.

As indicated in Table 14, LRT and the proposed tests control the Type I error but the proposed tests exhibit a fair yet insubstantial amount of power loss. The loss of power of the proposed test is primarily due to their smaller inference sample.

**B.2. Inflated Type I errors for holdout permutation test (HPT) and permutation test (PT)**

This subsection demonstrates that HPT and PT can incur inflated Type I errors. Specifically, we consider the same simulation setting in Section 6.2, with  $N = 2000$ ,  $B = 0.1$ ,

---

7. <https://gist.github.com/rnowling/ec9c9038e492d55ffae2ae257aa4acd9>

Test	sample size	Type I error	Power
One-split	500	0.040	(0.15, 0.20)
	800	0.020	(0.42, 0.44)
	1000	0.040	(0.69, 0.77)
Two-split	500	0.032	(0.13, 0.13)
	800	0.030	(0.18, 0.18)
	1000	0.020	(0.39, 0.34)
Comb. one-split	500	0.042	(0.19, 0.24)
	800	0.010	(0.53, 0.59)
	1000	0.019	(0.79, 0.85)
Comb. two-split	500	0.020	(0.06, 0.15)
	800	0.012	(0.32, 0.37)
	1000	0.002	(0.51, 0.50)
LRT	500	0.003	(0.52, 0.55)
	800	0.000	(0.92, 0.93)
	1000	0.035	(0.98, 0.99)

Table 14: Empirical Type I errors and powers of the likelihood ratio test, the one-split and two-split tests, and their combined tests at a nominal level  $\alpha = 0.05$ . The likelihood ratio uses the asymptotic  $\chi$ -square distribution for the null distribution.

$r = 0.85$ ,  $p = 100$ ,  $\tau = 2$ ,  $L = 2$ ,  $\varpi = 128$ , and  $|\mathcal{S}_0| = 3$ . The Type I errors of the null hypothesis based on  $\mathcal{S} = \{1, 2, 3\}$  for all tests are reported in Table 15 over 100 simulations. As indicated in Table 15, the one-split/two-split tests and their combined tests control Type I error, yet neither HPT nor PT could control the Type I error under a nominal level.

One-split	Two-split	Comb. one-split	Comb. two-split	HPT	PT
0.03	0.04	0.01	0.01	0.12	0.97

Table 15: Type I errors of the holdout permutation test (HPT), the permutation test (PT), the one-split and two-split tests and their combined tests at a nominal level  $\alpha = 0.05$ .

### B.3. Effect of size of grids of data-adaptive splitting scheme

This subsection demonstrates the effect of size of grids of the perturbation size  $\rho$  and the splitting ratio  $\zeta$  for the heuristic data-adaptive scheme in Section 5.2.

For illustration, we consider the same simulation setting as in Example 1 with  $N = 6000$ , then the grids  $\zeta = \{.2, .6\}$ ,  $\{.2, .4, .6, .8\}$ ,  $\{.2, .3, \dots, .9\}$ , and  $\rho = \{.01, .1, 1\}$ ,  $\{.01, .05, .1, .5, 1\}$  are examined. The Type I error and power functions for the proposed methods are summarized in Table 16.

As indicated in Table 16, Type I error, power and computation time based on data adaptive splitting method do not significantly affected by the grid sets of  $(\zeta, \rho)$  due to the early stopping mechanism in (13).

Test	$\zeta$	$\rho$	Type I error	Power	Time (Second)
One-split	{.2, .6}	{.01, .1, 1}	0.020	(0.65, 1.00, 1.00)	31.4(1.2)
		{.01, .05, .1, .5, 1}	0.022	(0.58, 1.00, 1.00)	30.4(1.1)
	{.2, .4, .6, .8}	{.01, .1, 1}	0.010	(0.62, 1.00, 1.00)	29.4(0.5)
		{.01, .05, .1, .5, 1}	0.050	(0.61, 0.99, 1.00)	41.2(0.3)
	{.2, .3, $\dots$ , .9}	{.01, .1, 1}	0.009	(0.63, 1.00, 1.00)	32.2(2.0)
		{.01, .05, .1, .5, 1}	0.021	(0.70, 1.00, 1.00)	32.1(1.2)
Two-split	{.2, .6}	–	0.032	(0.17, 0.49, 0.56)	30.6(0.6)
	{.2, .4, .6, .8}	–	0.035	(0.18, 0.51, 0.58)	37.0(0.2)
	{.2, .3, $\dots$ , .9}	–	0.031	(0.16, 0.58, 0.62)	30.3(0.7)

Table 16: Empirical Type I errors and powers of the one-split and two-split tests with different size of grids at a nominal level  $\alpha = 0.05$ .

### Appendix C. Technical proofs

In this section, we rewrite  $m$  as  $m_n$  to emphasize the monotonicity of  $m$  as a subsequence of  $n$ , that is,  $m_1 < \dots < m_n$ .

**Proof of Lemma 1.** We first prove that  $\mathbf{Y} \perp \mathbf{X}_S \mid \mathbf{X}_{S^c}$  yields  $R(f^*) - R_S(g^*) = 0$ . To find  $f^*$  and  $g^*$ , it suffices to consider the pointwise minimization of  $R(f)$  and  $R_S(g)$ , that is, for any  $\mathbf{x}$ , we have

$$\begin{aligned} f^*(\mathbf{x}) &= \operatorname{argmin}_u \mathbb{E}(l(u, \mathbf{Y}) \mid \mathbf{X}_S = \mathbf{x}_S, \mathbf{X}_{S^c} = \mathbf{x}_{S^c}) = \operatorname{argmin}_u \mathbb{E}(l(u, \mathbf{Y}) \mid \mathbf{X}_{S^c} = \mathbf{x}_{S^c}) \\ &= \operatorname{argmin}_u \mathbb{E}(l(u, \mathbf{Y}) \mid \mathbf{Z}(\mathbf{X}) = \mathbf{z}(\mathbf{x})) = g^*(\mathbf{z}(\mathbf{x})), \end{aligned}$$

where the second equality follows from the conditional independence. Therefore,  $R(f^*) = \mathbb{E}(l(f^*(\mathbf{X}), \mathbf{Y})) = \mathbb{E}(l(g^*(\mathbf{Z}(\mathbf{X})), \mathbf{Y})) = R_S(g^*)$ .

Next, we show that  $H_0$  is equivalent to conditional independence almost surely, if the cross-entropy loss  $l(f(\mathbf{X}), Y) = -\mathbf{1}_Y^\top \log(f(\mathbf{X}))$  is used in (1). Note that  $\mathbf{f}_k^*(\mathbf{x}) = \mathbb{P}(Y = k \mid \mathbf{X} = \mathbf{x})$  and  $\mathbf{g}_k^*(\mathbf{z}) = \mathbb{P}(Y = k \mid \mathbf{Z}(\mathbf{X}) = \mathbf{z}(\mathbf{x}))$ , we have

$$0 = R(f^*) - R_S(g^*) = \mathbb{E}\left(\mathbf{1}_Y^\top \log\left(\frac{\mathbf{f}^*(\mathbf{X})}{\mathbf{g}^*(\mathbf{Z}(\mathbf{X}))}\right)\right) = \mathbb{E}\left(\text{KL}(\mathbf{f}^*(\mathbf{X}), \mathbf{g}^*(\mathbf{Z}(\mathbf{X})))\right),$$

which yields that  $\text{KL}(\mathbf{f}^*(\mathbf{X}), \mathbf{g}^*(\mathbf{Z}(\mathbf{X}))) = 0$  with probability one, and  $\text{KL}(\cdot, \cdot)$  is the Kullback–Leibler divergence. Thus,  $\mathbf{f}^*(\mathbf{X}) = \mathbf{g}^*(\mathbf{Z}(\mathbf{X}))$  with probability one. This leads to the desirable results.  $\square$

**Proof of Theorems 2 and 8.** Note that  $\Lambda_n^{(l)} = T_{n,1}^{(l)} + T_{n,2}^{(l)} + T_{n,3}^{(l)}$ , where  $T_{n,1}^{(l)}$ ,  $T_{n,2}^{(l)}$ , and  $T_{n,3}^{(l)}$  are defined as

$$\begin{aligned} T_{n,1}^{(l)} &= \frac{(m_n^{(l)})^{1/2}}{\hat{\sigma}_n^{(l)}} \left( \frac{1}{m_n^{(l)}} \sum_{j=1}^{m_n^{(l)}} (\Delta_{n,j}^{(l)} - \mathbb{E}(\Delta_{n,j}^{(l)} \mid \mathcal{E}_n)) \right), \\ T_{n,2}^{(l)} &= \frac{(m_n^{(l)})^{1/2}}{\hat{\sigma}_n^{(l)}} \left( R(\hat{f}_n) - R(f^*) - (R_S(\hat{g}_n) - R_S(g^*)) \right), \\ T_{n,3}^{(l)} &= \frac{(m_n^{(l)})^{1/2}}{\hat{\sigma}_n^{(l)}} (R(f^*) - R_S(g^*)), \end{aligned}$$

Test	$L$	#Parameters	width $\varpi$	Type I error	Power	Time (Second)
One-split	2	3232	32	0.050	(0.26, 0.82, 0.84)	36.91(0.21)
		6464	64	0.041	(0.27, 0.84, 0.89)	35.48(0.17)
		12928	128	0.048	(0.22, 0.90, 0.91)	35.31(0.18)
	3	4256	32	0.054	(0.66, 1.00, 1.00)	39.44(0.29)
		10560	64	0.051	(0.65, 1.00, 1.00)	38.41(0.24)
		29312	128	0.050	(0.61, 0.99, 1.00)	41.24(0.29)
	4	5280	32	0.066	(0.98, 1.00, 1.00)	42.27(0.22)
		18752	64	0.048	(1.00, 1.00, 1.00)	41.81(0.30)
		62080	128	0.054	(0.99, 1.00, 1.00)	43.12(0.43)
Two-split	2	3232	32	0.050	(0.03, 0.16, 0.13)	35.76(0.20)
		6464	64	0.050	(0.04, 0.11, 0.13)	35.28(0.30)
		12928	128	0.055	(0.05, 0.14, 0.16)	33.65(0.16)
	3	4256	32	0.044	(0.19, 0.63, 0.63)	37.19(0.20)
		10560	64	0.035	(0.16, 0.47, 0.62)	35.82(0.20)
		29312	128	0.035	(0.18, 0.51, 0.58)	37.02(0.16)
	4	5280	32	0.044	(0.54, 1.00, 1.00)	43.54(0.34)
		18752	64	0.041	(0.54, 1.00, 1.00)	40.28(0.26)
		62080	128	0.045	(0.54, 1.00, 1.00)	47.07(0.31)
Comb. one-split	2	3232	32	0.046	(0.39, 0.98, 0.94)	61.99(0.17)
		6464	64	0.022	(0.22, 0.97, 0.97)	61.40(0.16)
		12928	128	0.020	(0.40, 1.00, 1.00)	60.42(0.45)
	3	4256	32	0.049	(0.80, 1.00, 1.00)	63.71(0.21)
		10560	64	0.032	(0.79, 1.00, 1.00)	65.23(0.14)
		29312	128	0.046	(0.86, 1.00, 1.00)	68.28(0.26)
	4	5280	32	0.054	(1.00, 1.00, 1.00)	145.38(0.73)
		18752	64	0.032	(1.00, 1.00, 1.00)	112.77(1.15)
		62080	128	0.032	(1.00, 1.00, 1.00)	127.07(0.79)
Comb. two-split	2	3232	32	0.022	(0.00, 0.08, 0.11)	30.32(0.12)
		18752	64	0.015	(0.06, 0.09, 0.15)	31.73(0.10)
		12928	128	0.017	(0.04, 0.13, 0.08)	33.44(0.12)
	3	4256	32	0.011	(0.08, 0.75, 0.76)	41.46(0.34)
		10560	64	0.007	(0.08, 0.66, 0.67)	34.27(0.27)
		29312	128	0.030	(0.10, 0.70, 0.65)	76.28(0.54)
	4	4256	32	0.013	(0.65, 1.00, 1.00)	48.99(0.61)
		18752	64	0.025	(0.65, 1.00, 1.00)	39.13(0.07)
		62080	128	0.014	(0.69, 1.00, 1.00)	49.05(0.15)

Table 17: Type I errors and powers of the one-split and two-split tests and their combined tests in Example 3 at a nominal level  $\alpha = 0.05$ .

where  $m_n^{(l)} = m_n$  if  $l = 1$  and  $m_n^{(l)} = m_n/2$  if  $l = 2$ , and  $T_{n,3}^{(1)} = T_{n,3}^{(2)} = 0$  under  $H_0$ .

Test	$B$	$(L, d)$	Comb. method	Type I error	Power
Comb. one-split	0.20	(3, 128)	Hommel	0.019	(0.27, 0.93, 0.93)
			Bonferroni	0.044	(0.43, 0.95, 0.98)
			1 <sup>st</sup> -Quantile	0.004	(0.13, 0.89, 0.95)
			median	0.000	(0.02, 0.69, 0.75)
			Cauchy	0.050	(0.41, 1.00, 1.00)
			harmonic	0.014	(0.20, 0.84, 0.94)
Comb. one-split	0.40	(4, 32)	Hommel	0.054	(1.00, 1.00, 1.00)
			Bonferroni	0.097	(1.00, 1.00, 1.00)
			1 <sup>st</sup> -Quantile	0.011	(1.00, 1.00, 1.00)
			median	0.000	(1.00, 1.00, 1.00)
			Cauchy	0.099	(1.00, 1.00, 1.00)
			harmonic	0.035	(1.00, 1.00, 1.00)

Table 18: Empirical Type I errors and powers of the different combined methods for the one-split test in Example 6 at a nominal level  $\alpha = 0.05$ .

Now consider  $T_{n,1}^{(l)}$  and  $T_{n,2}^{(l)}$  separately. To proceed, we first show that  $\hat{\sigma}_n^{(1)} \xrightarrow{p} \sigma^{(1)}$  and  $\hat{\sigma}_n^{(2)} \xrightarrow{p} \sigma^{(2)}$ . Specifically, for  $l = 1, 2$ ,

$$\begin{aligned}
(\hat{\sigma}_n^{(l)})^2 &= \frac{m_n^{(l)}}{m_n^{(l)} - 1} \left( \frac{1}{m_n^{(l)}} \sum_{j=1}^{m_n^{(l)}} (\Delta_{n,j}^{(l)})^2 - \left( \frac{1}{m_n^{(l)}} \sum_{j=1}^{m_n^{(l)}} \Delta_{n,j}^{(l)} \right)^2 \right) \\
&= \frac{m_n^{(l)}}{m_n^{(l)} - 1} \left( \frac{1}{m_n^{(l)}} \sum_{j=1}^{m_n^{(l)}} ((\Delta_{n,j}^{(l)})^2 - \mathbb{E}((\Delta_{n,j}^{(l)})^2 | \mathcal{E}_n)) \right) \\
&\quad + \frac{m_n^{(l)}}{m_n^{(l)} - 1} \left( \left( \frac{1}{m_n^{(l)}} \sum_{j=1}^{m_n^{(l)}} (\mathbb{E}(\Delta_{n,j}^{(l)} | \mathcal{E}_n) - \Delta_{n,j}^{(l)}) \right) \left( \frac{1}{m_n^{(l)}} \sum_{j=1}^{m_n^{(l)}} (\mathbb{E}(\Delta_{n,j}^{(l)} | \mathcal{E}_n) + \Delta_{n,j}^{(l)}) \right) \right) \\
&\quad + \frac{m_n^{(l)}}{m_n^{(l)} - 1} \left( \text{Var}(\Delta_n^{(l)} | \mathcal{E}_n) \right) \xrightarrow{p} (\sigma^{(l)})^2,
\end{aligned}$$

which follows from the continuous mapping theorem, Assumption C for the one-split test or Assumption C' for the two-split test, and the fact that

$$\frac{1}{m_n^{(l)}} \sum_{j=1}^{m_n^{(l)}} (\Delta_{n,j}^{(l)} - \mathbb{E}(\Delta_{n,j}^{(l)} | \mathcal{E}_n)) \xrightarrow{p} 0, \quad \frac{1}{m_n^{(l)}} \sum_{j=1}^{m_n^{(l)}} ((\Delta_{n,j}^{(l)})^2 - \mathbb{E}((\Delta_{n,j}^{(l)})^2 | \mathcal{E}_n)) \xrightarrow{p} 0,$$

which are obtained from the law of large number of the triangular array  $\{\Delta_{n,j}^{(l)}\}_{1 \leq j \leq m_n}$  and Assumptions B and B', c.f., Corollary 9.5.6 of (Cappé et al., 2006).

Consequently, when  $m = o(n^{2\gamma})$ , it follows from Assumption A and  $\hat{\sigma}_n^{(l)} \xrightarrow{p} \sigma^{(l)} > 0$  that

$$T_{n,2}^{(l)} = \frac{\sqrt{m_n}}{\hat{\sigma}_n^{(l)}} \left( R(\hat{f}_n) - R(f^*) - (R_S(\hat{g}_n) - R_S(g^*)) \right) \xrightarrow{p} 0.$$

Moreover,

$$T_{n,1}^{(l)} = \frac{\sigma^{(l)}}{\hat{\sigma}_n^{(l)}} \frac{1}{(m_n^{(l)})^{1/2} \sigma^{(l)}} \left( \sum_{j=1}^{m_n^{(l)}} (\Delta_{n,j}^{(l)} - \mathbb{E}(\Delta_{n,j}^{(l)} | \mathcal{E}_n)) \right) \xrightarrow{d} N(0, 1), \quad (19)$$

which follows from the continuous mapping theorem, Slutsky's Lemma, and the central limit Theorem of the triangular array  $\{\Delta_{n,j}^{(l)}\}_{1 \leq j \leq m_n^{(l)}}$ , and Assumptions B or B', c.f., Corollary 9.5.11 of (Cappé et al., 2006). The desired result then follows. This completes the proof.  $\square$

**Proof of Theorems 3 and 9.** For  $q$ -order combined tests, let  $A = \{\bar{P}^{(l)} \leq \alpha\}$  and  $B = \{\sum_{u=1}^U \mathbb{I}(P_u^{(l)} \leq \frac{q\alpha}{U}) \geq q\}$ . Since  $A = \{P_{(q)}^{(l)} \leq \frac{q\alpha}{U}\} = B$ , by Markov's inequality, it follows from the assumptions that either Theorem 2 or Theorem 8 holds. Hence,

$$\mathbb{P}(A|H_0) = \mathbb{P}(B|H_0) \leq \frac{\sum_{u=1}^U \mathbb{P}(P_u^{(l)} \leq \frac{q\alpha}{U} | H_0)}{q} \rightarrow \frac{U \mathbb{P}(\Phi(Z) \leq \frac{q\alpha}{U})}{q} = \alpha, \text{ as } n \rightarrow \infty,$$

where  $Z$  follows  $N(0, 1)$ ,  $\Phi(Z)$  follows the uniform distribution on  $[0, 1]$ , and the last equality follows from continuous mapping theorem.

For Hommel combined test, according to the proof of 3.3 in (Hommel, 1983), when  $n \rightarrow \infty$ , we have

$$\mathbb{P}(\bar{P}^{(l)} \leq \alpha | H_0) \leq \sum_{i=1}^{U-1} \frac{1}{i(i+1)} \sum_{u=1}^U \mathbb{P}(P_u^{(l)} \leq \frac{\alpha i}{C_U U} | H_0) + \frac{1}{U} \sum_{u=1}^U \mathbb{P}(P_u^{(l)} \leq \frac{\alpha}{C_U} | H_0) \rightarrow \alpha.$$

This completes the proof.  $\square$

**Proof of Theorems 4 and 10.** Let  $\delta^{(1)} = \delta$  and  $\delta^{(2)} = \delta/\sqrt{2}$ , using the same argument in the proof of Theorems 2 and 8, we have that  $T_{n,2}^{(l)} \xrightarrow{p} 0$  when  $m = o(n^{2\gamma})$ , and  $T_{n,1}^{(l)} \xrightarrow{d} N(0, 1)$ . Note that  $T_{n,3}^{(l)} = \frac{\sqrt{m_n^{(l)}}}{\hat{\sigma}_n^{(l)}} (R(f^*) - R_S(g^*)) = -\delta^{(l)}/\hat{\sigma}_n^{(l)}$ . By Slutsky's theorem, we have

$$\Lambda_n^{(1)} \xrightarrow{d} N(-\delta^{(1)}/\sigma^{(1)}, 1), \quad \Lambda_n^{(2)} \xrightarrow{d} N(-\delta^{(2)}/\sigma^{(2)}, 1). \quad (20)$$

Consequently,

$$\liminf_{n \rightarrow \infty} \pi_n^{(l)}(\delta) = \Phi\left(\frac{\delta^{(l)}}{\sigma^{(l)}} - z_\alpha\right); \quad l = 1, 2.$$

The desired result then follows. This completes the proof.  $\square$

**Proof of Theorems 5 and 11.** Denote  $\delta^{(1)} = \delta$  and  $\delta^{(2)} = \delta/\sqrt{2}$ . We first prove for  $q$ -order combined tests. Note that  $\bar{\pi}_n^{(l)}(\delta) = 1 - \mathbb{P}(\bar{P}^{(l)} \geq \alpha | H_a)$ . By Markov's inequality, Type II error is upper bounded by  $\mathbb{P}(\bar{P}^{(l)} \geq \alpha | H_a) \leq \min\left(\frac{U}{\alpha q} \mathbb{E}(P_{(q)}^{(l)} | H_a), 1\right)$ . To bound the expectation of an order statistic based on dependent samples, we apply (1) of (Bertsimas et al., 2006), which is a version of (Arnold et al., 1979):

$$\mathbb{E}(P_{(q)}^{(l)} | H_a) \leq \bar{\mu} + \left( \frac{q-1}{U-q+1} \sum_{u=1}^U (\sigma_u^2 + (\mu_u - \bar{\mu})^2) \right)^{1/2}, \quad (21)$$

where  $\bar{\mu} = U^{-1} \sum_{u=1}^U \mu_u$ ,  $\mu_u = \mathbb{E}(P_u^{(l)} | H_a)$  and  $\sigma_u^2 = \text{Var}(P_u^{(l)} | H_a)$ .

For  $u = 1, \dots, U$ , by (20) and Portmanteau's theorem,  $\mathbb{E}(P_u^{(l)}|H_a) \rightarrow \mathbb{E}(\Phi(Z - \frac{\delta^{(l)}}{\sigma^{(l)}}))$  as  $n \rightarrow \infty$ . By Corollary 1 of (Ellison, 1964),  $\mathbb{E}(\Phi(Z - \frac{\delta^{(l)}}{\sigma^{(l)}})) = \Phi(-\frac{\delta^{(l)}}{\sqrt{2}\sigma^{(l)}})$ . Similarly,  $\text{Var}(P_u^{(l)}|H_a) \rightarrow \text{Var}(\Phi(Z - \frac{\delta^{(l)}}{\sigma^{(l)}}))$ ;  $u = 1, \dots, U$ ;  $\text{Var}(\Phi(Z - \frac{\delta^{(l)}}{\sigma^{(l)}})) = \Phi(-\frac{\delta^{(l)}}{\sqrt{2}\sigma^{(l)}}) - \Phi^2(-\frac{\delta^{(l)}}{\sqrt{2}\sigma^{(l)}}) - 2T(-\frac{\delta^{(l)}}{\sqrt{2}\sigma^{(l)}}, \frac{\sqrt{3}}{3})$ , where  $T(\cdot, \cdot)$  is Owen's  $T$  function (Owen, 1956).

Therefore, by (21), as  $n \rightarrow \infty$ ,

$$\begin{aligned} \mathbb{E}(P_u^{(l)}|H_a) &\rightarrow \mathbb{E}(\Phi(Z - \frac{\delta^{(l)}}{\sigma^{(l)}})) + \left( \frac{q-1}{U-q+1} \text{Var}(\Phi(Z - \frac{\delta^{(l)}}{\sigma^{(l)}})) \right)^{1/2} \\ &= \Phi(-\frac{\delta^{(l)}}{\sqrt{2}\sigma^{(l)}}) + \sqrt{\frac{q-1}{U-q+1}} \left( \Phi(\frac{\delta^{(l)}}{\sqrt{2}\sigma^{(l)}}) - \Phi^2(\frac{\delta^{(l)}}{\sqrt{2}\sigma^{(l)}}) - 2T(-\frac{\delta^{(l)}}{\sqrt{2}\sigma^{(l)}}, \frac{\sqrt{3}}{3}) \right)^{1/2}. \end{aligned}$$

The desired result then follows. Therefore, for Hommel combined test,

$$\mathbb{P}(C_U \min_{1 \leq q \leq U} \frac{U}{q} P_{(q)}^{(l)} \leq \alpha | H_a) \geq \max_{1 \leq q \leq U} \mathbb{P}(\frac{U}{q} P_{(q)}^{(l)} \leq \frac{\alpha}{C_U} | H_a).$$

The desired result then follows by taking limits for both sides. This completes the proof.  $\square$

**Proof of Lemma 6.** To proceed, let  $f_0 \in \mathcal{H}$  be a neural network, and its weight matrix is exactly same with that of  $g_0$  defined in (9), expect that  $j$ -th ( $j \in \mathcal{S}_0$ ) column in the first layer is set as zero, which implies that  $f^*(\mathbf{X}) = f_0(\mathbf{X}) = g_0(\mathbf{Z}(\mathbf{X}))$ .

To verify Assumption A, it suffices to verify the entropy condition of  $\mathcal{H}$ . By Theorem 3.3 of (Bartlett et al., 2017), for any  $\omega > 0$ , we have

$$\log \mathcal{N}(u, \mathcal{H}, \|\cdot\|_2) \leq \log \left( \frac{p \log(2\varpi^2)}{u^2} \tau^{2L} \right) \leq c(p, \varpi, \tau, L) \log(u^{-1}) = O(u^{-\omega}),$$

where  $\mathcal{N}(u, \mathcal{H}, \|\cdot\|_2)$  is the covering number based on  $L_2$ -norm,  $c(p, \varpi, \tau, L)$  is a constant depends on  $p, \varpi, \tau$ , and  $L$ . By (Han et al., 2019),

$$\begin{aligned} R(\hat{f}_n) - R(f^*) &= \mathbb{E}(\hat{f}_n(\mathbf{X}) - f^*(\mathbf{X}))^2 = O_p(n^{-1+\omega}), \\ R_{\mathcal{S}}(\hat{g}_n) - R_{\mathcal{S}}(g^*) &= \mathbb{E}(\hat{g}_n(\mathbf{X}) - g^*(\mathbf{X}))^2 = O_p(n^{-1+\omega}). \end{aligned} \quad (22)$$

Therefore,  $\gamma = 1 - \omega$  for Assumption A with any  $\omega > 0$ . Then Assumptions B and B' follow from the fact that  $f \in \mathcal{H}$  is upper bounded by a constant, that is

$$\sup_{\mathbf{x} \in [-1, 1]^d} |f(\mathbf{x})| = \sup_{\mathbf{x} \in [-1, 1]^d} |A(\mathbf{W}^L \cdots A(\mathbf{W}^1 \mathbf{x}))| \leq \left( \prod_{l=1}^L \|\mathbf{W}^l\|_2 \right) \sup_{\mathbf{x} \in [-1, 1]^d} \|\mathbf{x}\|_2 \leq \sqrt{p} \tau^L, \quad (23)$$

where the second last inequality follows from the definition of the matrix norm. Next, we verify Assumptions C and C'. Let  $\mathbb{E}_n(\cdot) = \mathbb{E}(\cdot | \mathcal{E}_n)$ ,  $\text{Var}_n(\cdot) = \text{Var}(\cdot | \mathcal{E}_n)$ ,  $\Psi(f, g, \mathbf{U}) = l(f(\mathbf{X}), Y) - l(g(\mathbf{Z}(\mathbf{X})), Y)$ , and  $\mathbf{U} = (\mathbf{X}, Y)$ . Then,

$$\begin{aligned} \text{Var}_n(\Delta_{n,1}^{(1)}) &= \text{Var}_n(\Psi(\hat{f}_n, \hat{g}_n, \mathbf{U})) + \rho_n^2 \\ &= \text{Var}_n(\Psi(\hat{f}_n, f^*, \mathbf{U}) + \Psi(f^*, g^*, \mathbf{U}) + \Psi(g^*, \hat{g}_n, \mathbf{U})) + \rho_n^2 \\ &= \text{Var}_n(\Psi(\hat{f}_n, \hat{g}_n, \mathbf{U})) + \text{Var}_n(\Psi(f^*, g^*, \mathbf{U})) + \text{Var}_n(\Psi(g^*, \hat{g}_n, \mathbf{U})) \\ &\quad + 2 \text{Cov}(\Psi(\hat{f}_n, \hat{g}_n, \mathbf{U}), \Psi(f^*, g^*, \mathbf{U})) + 2 \text{Cov}(\Psi(\hat{f}_n, \hat{g}_n, \mathbf{U}), \Psi(g^*, \hat{g}_n, \mathbf{U})) \\ &\quad + 2 \text{Cov}(\Psi(f^*, g^*, \mathbf{U}), \Psi(g^*, \hat{g}_n, \mathbf{U})) + \rho_n^2 \xrightarrow{p} \text{Var}(\Psi(f^*, g^*, \mathbf{U})) + \rho_n^2 = (\sigma^{(1)})^2, \end{aligned}$$



where the last equality follows from the uniform boundedness of  $\mathcal{H}$  in (23) and the fact that  $\text{Var}_n(\Psi(g^*, \hat{g}_n, \mathbf{U})), \text{Var}_n(\Psi(\hat{f}_n, f^*, \mathbf{U})) \xrightarrow{p} 0$ . Specifically,

$$\begin{aligned} \text{Var}_n(\Psi(\hat{f}_n, f^*, \mathbf{U})) &\leq \mathbb{E}_n(\Psi^2(\hat{f}_n, f^*, \mathbf{U})) = \mathbb{E}_n\left((\hat{f}_n(\mathbf{X}) - f^*(\mathbf{X}))^2(\hat{f}_n(\mathbf{X}) + f^*(\mathbf{X}) - 2Y)^2\right) \\ &\leq (2\sqrt{p}\tau + 4\varsigma^2)\mathbb{E}_n\left((\hat{f}_n(\mathbf{X}) - f^*(\mathbf{X}))^2\right) = (2\sqrt{p}\tau + 4\varsigma^2)(R(\hat{f}_n) - R(f^*)) \xrightarrow{p} 0. \end{aligned}$$

Similarly, we can show that  $\text{Var}_n(\Psi(g^*, \hat{g}_n, \mathbf{U})) \xrightarrow{p} 0$ .

Moreover, for  $\Delta_n^{(2)}$ , using the same argument, we have

$$\begin{aligned} \text{Var}_n(\Delta_n^{(2)}) &= \text{Var}_n(l(\hat{f}_n(\mathbf{X}), Y) - l(\hat{g}_n(\mathbf{Z}'), Y')) = \text{Var}_n(l(\hat{f}_n(\mathbf{X}), Y)) + \text{Var}_n(l(\hat{g}_n(\mathbf{Z}), Y)) \\ &\xrightarrow{p} \text{Var}(l(f^*(\mathbf{X}), Y)) + \text{Var}(l(g^*(\mathbf{Z}), Y)) = (\sigma^{(2)})^2. \end{aligned}$$

The desired result then follows. This completes the proof.  $\square$

**Proof of Lemma 7.** By the definitions of  $n$  and  $m$  in (11), we have

$$m = N - n \leq N - x_0 = N_0 \log(x_0)/2 / \log(N_0/2) = o(n^{2\gamma}),$$

where  $\gamma > 0$  is any fixed constant in Assumption A, and the last equality follows from  $n \geq x_0$ . This completes the proof.  $\square$

## References

- Barry C Arnold, Richard A Groeneveld, et al. Bounds on expectations of linear systematic statistics based on dependent samples. *Annals of Statistics*, 7(1):220–223, 1979.
- Peter L Bartlett, Dylan J Foster, and Matus J Telgarsky. Spectrally-normalized margin bounds for neural networks. In *Advances in Neural Information Processing Systems*, pages 6240–6249, 2017.
- Thomas B Berrett, Yi Wang, Rina Foygel Barber, and Richard J Samworth. The conditional permutation test for independence while controlling for confounders. *Journal of the Royal Statistical Society: Series B (Statistical Methodology)*, 2019.
- Dimitris Bertsimas, Karthik Natarajan, and Chung-Piaw Teo. Tight bounds on expected order statistics. *Probability in the Engineering and Informational Sciences*, 20(4):667, 2006.
- Leo Breiman. Random forests. *Machine Learning*, 45(1):5–32, 2001.
- Adolf Buse. The likelihood ratio, wald, and lagrange multiplier tests: An expository note. *The American Statistician*, 36(3a):153–157, 1982.
- Emmanuel Candès, Yingying Fan, Lucas Janson, and Jinchi Lv. Panning for gold: Model-x knockoffs for high dimensional controlled variable selection. *Journal of the Royal Statistical Society: Series B (Statistical Methodology)*, 80(3):551–577, 2018.
- Olivier Cappé, Eric Moulines, and Tobias Rydén. *Inference in hidden Markov models*. Springer Science & Business Media, 2006.

- Victor Chernozhukov, Denis Chetverikov, Mert Demirer, Esther Duflo, Christian Hansen, Whitney Newey, and James Robins. Double/debiased machine learning for treatment and structural parameters, 2018.
- Yadolah Dodge and Daniel Commenges. *The Oxford dictionary of statistical terms*. Oxford University Press on Demand, 2006.
- Bradley Efron. Bootstrap methods: another look at the jackknife. In *Breakthroughs in statistics*, pages 569–593. Springer, 1992.
- Bob E Ellison. Two theorems for inferences about the normal distribution with applications in acceptance sampling. *Journal of the American Statistical Association*, 59(305):89–95, 1964.
- Ludwig Fahrmeir, Thomas Kneib, Stefan Lang, and Brian Marx. *Regression*. Springer, 2007.
- Julian J Faraway. Data splitting strategies for reducing the effect of model selection on inference. *Comput Sci Stat*, 30:332–41, 1998.
- Rong Ge, Furong Huang, Chi Jin, and Yang Yuan. Escaping from saddle points—online stochastic gradient for tensor decomposition. In *Conference on Learning Theory*, pages 797–842, 2015.
- Ian Goodfellow, Yoshua Bengio, and Aaron Courville. *Deep learning*. MIT press, 2016.
- Qiyang Han, Jon A Wellner, et al. Convergence rates of least squares regression estimators with heavy-tailed errors. *Annals of Statistics*, 47(4):2286–2319, 2019.
- Godfrey Harold Hardy, John Edensor Littlewood, George Pólya, György Pólya, DE Littlewood, et al. *Inequalities*. Cambridge university press, 1952.
- Gerhard Hommel. Tests of the overall hypothesis for arbitrary dependence structures. *Biometrical Journal*, 25(5):423–430, 1983.
- Daniel S Kermany, Michael Goldbaum, Wenjia Cai, Carolina CS Valentim, Huiying Liang, Sally L Baxter, Alex McKeown, Ge Yang, Xiaokang Wu, Fangbing Yan, et al. Identifying medical diagnoses and treatable diseases by image-based deep learning. *Cell*, 172(5):1122–1131, 2018.
- Gary King. *Unifying political methodology: The likelihood theory of statistical inference*. Cambridge University Press, 1989.
- Michael Kohler and Adam Krzyżak. Adaptive regression estimation with multilayer feed-forward neural networks. *Nonparametric Statistics*, 17(8):891–913, 2005.
- Michael Kohler and Adam Krzyżak. Nonparametric regression based on hierarchical interaction models. *IEEE Transactions on Information Theory*, 63(3):1620–1630, 2016.
- Yann LeCun, Léon Bottou, Yoshua Bengio, and Patrick Haffner. Gradient-based learning applied to document recognition. *Proceedings of the IEEE*, 86(11):2278–2324, 1998.

- Jing Lei, Max G'Sell, Alessandro Rinaldo, Ryan J Tibshirani, and Larry Wasserman. Distribution-free predictive inference for regression. *Journal of the American Statistical Association*, 113(523):1094–1111, 2018.
- Daniel F McCaffrey and A Ronald Gallant. Convergence rates for single hidden layer feedforward networks. *Neural Networks*, 7(1):147–158, 1994.
- Nicolai Meinshausen, Lukas Meier, and Peter Bühlmann. P-values for high-dimensional regression. *Journal of the American Statistical Association*, 104(488):1671–1681, 2009.
- Markus Ojala and Gemma C Garriga. Permutation tests for studying classifier performance. *Journal of Machine Learning Research*, 11(Jun):1833–1863, 2010.
- Donald B Owen. Tables for computing bivariate normal probabilities. *Annals of Mathematical Statistics*, 27(4):1075–1090, 1956.
- Maxim Raginsky, Alexander Rakhlin, and Matus Telgarsky. Non-convex learning via stochastic gradient langevin dynamics: a nonasymptotic analysis. *arXiv preprint arXiv:1702.03849*, 2017.
- J Romano and Cyrus DiCiccio. Multiple data splitting for testing. Technical report, Technical report, 2019.
- David E Rumelhart, Geoffrey E Hinton, and Ronald J Williams. Learning representations by back-propagating errors. *nature*, 323(6088):533–536, 1986.
- Jürgen Schmidhuber. Deep learning in neural networks: An overview. *Neural networks*, 61: 85–117, 2015.
- Johannes Schmidt-Hieber et al. Nonparametric regression using deep neural networks with relu activation function. *Annals of Statistics*, 48(4):1875–1897, 2020.
- Wesley Tansey, Victor Veitch, Haoran Zhang, Raul Rabadan, and David M Blei. The hold-out randomization test: Principled and easy black box feature selection. *arXiv preprint arXiv:1811.00645*, 2018.
- Vladimir Vovk and Ruodu Wang. Combining  $p$ -values via averaging. *Biometrika*, 2018.
- Larry Wasserman. *All of nonparametric statistics*. Springer Science & Business Media, 2006.
- Larry Wasserman and Kathryn Roeder. High dimensional variable selection. *Annals of statistics*, 37(5A):2178, 2009.
- Larry Wasserman, Aaditya Ramdas, and Sivaraman Balakrishnan. Universal inference. *Proceedings of the National Academy of Sciences*, 117(29):16880–16890, 2020.
- Lei Wu, Chao Ma, and E Weinan. How sgd selects the global minima in over-parameterized learning: A dynamical stability perspective. In *Advances in Neural Information Processing Systems*, pages 8279–8288, 2018.

Wei Zhang et al. Shift-invariant pattern recognition neural network and its optical architecture. In *Proceedings of Annual Conference of the Japan Society of Applied Physics*, 1988.